MEMOIRE DE FIN D'ETUDES

Caractérisation spatio-temporelle de l'aléa inondation dans les bassins versants naturels européens

Flood drivers across time and space in European catchments

Manal LAM'BARKI
Promotion Dakar

Mémoire présenté pour l'obtention du diplôme d'Ingénieur de l'ENGEES
Stage réalisé du 3 Janvier au 30 Juin 2022

Encadrant : Dr. René Orth

Abstract

Deriving the mechanisms that cause river floods is a key to understanding present and future flood risk. Studies that classify catchments according to their flood generating mechanisms in Europe often rely on inferences based on future changes or seasonality of processes. The present study presents a quantitative overview of flood-causing mechanisms throughout Europe based on a method using formal attributions of potential drivers to high flow peaks on an event-by-event basis.

The study also investigates the spatial and temporal variations in flood drivers by considering different time windows and seasons for floods. The method presented also considers a wider range of potential flood drivers.

Applying this method to a European runoff dataset of near-natural catchments reveals that antecedent rainfall is a prominent flood driver. However, the diverse patterns identified in flood generating mechanisms also show that floods cannot be caused by only one mechanism in the region. The results highlight the need for improved process understanding in flood risk assessment and predictions.

Résumé

Déterminer les mécanismes à l'origine des inondations fluviales est un élément clé pour comprendre les risques d'inondation actuels et futurs. Les études qui classent les bassins versants en fonction des processus qui génèrent les inondations en Europe s'appuient souvent sur des déductions basées sur les changements futurs ou la saisonnalité des mécanismes. La présente étude fournit un aperçu quantitatif des mécanismes générateurs d'inondations dans toute l'Europe, basé sur une méthode utilisant des attributions formelles de facteurs potentiels aux pics de débit élevés.
L'étude examine également les variations spatiales et temporelles des facteurs d'inondation en considérant différentes échelles temporelles pour les inondations. La méthode présentée prend également en compte un plus large éventail de facteurs potentiels d'inondation.
L'application de cette méthode à un ensemble de données de ruissellement européen de bassins versants naturels ou quasi-naturels révèle que les précipitations sont des facteurs qui favorisent les inondations. Cependant, la diversité d’autres facteurs identifiés dans les mécanismes de génération des inondations montre également que les inondations ne peuvent pas être causées par un seul mécanisme. Les résultats soulignent la nécessité d'améliorer la compréhension des processus dans l'évaluation et la prévision des risques d'inondation.

Table of contents

List of figures

List of tables

I. Introduction

A. From catchment to large-scale hydrology

In his 1931 seminal paper on the scope of hydrology, Horton defines any natural exposed surface as a unit area on which the hydrological cycle operates. From water flowing in porous media such as soils to the terrestrial water cycle, hydrological processes occur over many different scales interconnected in space and time. For example, river catchments, although bounded by defined natural limits where water is collected, are driven by meteorological inputs of water. The climate has long been recognized as the dominant control on the long-term water balance of catchments (Budyko, 1974). Many studies have investigated the complex links between streamflow metrics (annual regimes, low and high flows) and the atmospheric circulation using various circulation indices, air masses and atmospheric pressure fields (Hannah et al, 2014).

Moreover, it has been shown that watershed soil properties impact the long-term water balance by influencing the infiltration excess runoff (Potter et al., 2005). In regions where climatic demand for water (e.g., potential evapotranspiration) and climatic supply of water (e.g., precipitation) are out of phase, the consideration of the soil moisture and groundwater storage capacity can improve the estimation of the annual water balance (Wolock and McCabe, 1999).

This demonstrates the importance of integrating both large-scale climate interactions and catchment properties when understanding river regimes and their extremes under current and future conditions. A large-scale approach implies that the focus is not put on single-site linkings between atmospheric and local properties, but rather on larger and more general spatial patterns.

This perspective is needed to hypothesize and develop an understanding of the first order drivers of river flow at any given location (Kingston et al, 2020).

However, given the increasing concern about the impact of climate change on the hydrological cycle for both the supply and demand (Döll, 2002, 2009), it is crucial to go beyond the catchment scale to identify possible spatial patterns and drivers of widespread hydrological processes, including hydrometeorological extremes. Gupta et al. (2014) advocates for taking further advantage of the extensive data sets now available (Schaake et al, 2001; orth et al, 2015; GRDC, 2015; Stahl et al, 2010) and to follow a large-sample approach to hydrological investigation in order to “balance depth with breadth”. This holistic approach can increase the ability to establish general hydrologic concepts applicable across different regions.

B. On hydrological extremes

1. Definitions

Hydrological extremes occur in many regions of the globe, making them a relevant phenomenon with significant impacts on society (Kundzewicz and Kaczmarek, 2000; Orth et al, 2022). Droughts and flood-related disasters have been more devastating than other natural hazards (volcanoes, earthquakes, landslides, etc.) in terms of potential socio-economic damage (Barredo, 2007; Naumann et al, 2015; Gao et al, 2019), due to their often-large spatial extent and high societal impact. High and low flows and associated floods and hydrological droughts are mainly caused by meteorological anomalies and modulated by catchment processes and human activities (Manfreda et al, 2018). They both occur on different spatial and temporal scales with floods primarily occurring between a river-basin scale to a regional scale and between a daily and monthly temporal scale. They also happen within the temporal scale of an individual event, rather than on seasonal basis, as opposed to droughts which can occur seasonally (Figure 1).

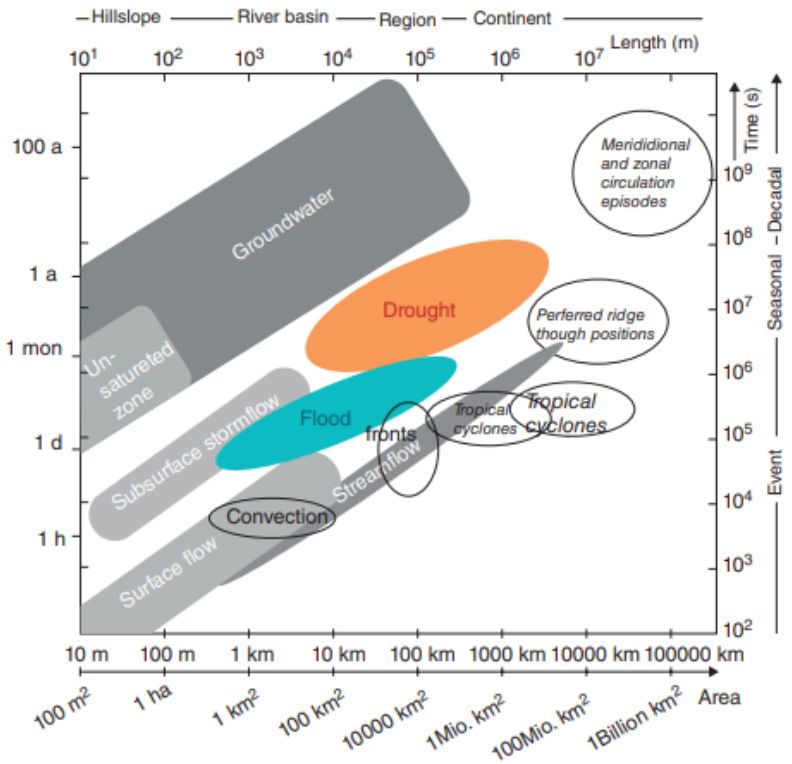

Figure 1 : Spatial and temporal scales of hydrological processes including floods and droughts (after Stahl and Hisdal , 2004)

While droughts can occur in all parts of the hydrological cycle (precipitation, soil moisture, groundwater or streamflow), floods are mainly limited to abnormally high levels in streamflow or precipitation. In that sense, river flow is the hydrological variable of most common importance as episodes of low or high streamflow can be identified in the framework of a threshold-crossing. It is important to note that there are several challenges when studying river floods: i) there is no uniform and broadly agreed upon definition of floods as such notions always involve a degree of subjectivity and arbitrariness of a chosen threshold. As no unique definition of such a threshold exists, flood event separation techniques can be

defined by the objectives of the flood analyses, e.g., by the beginning of specific areas of inundations, navigation problems or by a significant deviation from the normal hydrologic conditions of an area (Fischer et al, 2021). Inundated area is also another direct determining characteristic, as opposed to droughts where the starting date is more important, as winter low flows can have lesser impacts in the vegetation (Kundzewicz and Kaczmarek, 2000).

ii) An "abnormally" large or low discharge can be difficult to pin down, particularly within a timeframe. When measuring flood peaks, the issue of required frequent measurements arises as many measurements are done during periods of low or medium flow but very few during flood events due to the danger of streamflow gauging during a flood event, if measurements are not automatized (Davie, 2019).

Moreover, floods should be defined in a way that encompasses not just inundation and devastation, but also goes beyond river flood definitions: for example, by Chow (1956): "A flood is a relatively high flow which overtops the natural waterway defined by the river". Ward (1978) defines floods as a body of water which rises to overflow land which is not normally submerged. This definition reflects the spatially diverse types of floods such as river, coastal or urban floods. The definition of floods should also incorporate the notion of risk given the amount the economic damage that they cause. The latter also depends on the location of the inundation as the cost of damage of floodings in urban areas with large infrastructures is often larger than in agricultural lands.

Flood risk is defined as the product of the probability and consequences of flooding. One way to represent the spatial distribution of flood risk are maps (Merz et al, 2007). They can be classified into three categories: flood hazard maps, that show the intensity of floods and their associated exceedance probability; flood vulnerability maps, which illustrate the consequences of floods; and flood risk maps, showing the spatial distribution of the risk (Di Baldassarre, 2012). Floodplain maps of the inundation area are one of the most common categories of map used to illustrate flood hazard (Bates et al., 2004).

In addition to in-situ flood monitoring, remote sensing measurements have been able to detect anomalies in surface water and map in near-real time major floods using passive microwave satellite observations (Bjerklie et al, 2003; Global Floods Detection System).

2. Hydrological extremes in a changing climate

Considering that non-stationarity (e.g., changing properties in time) will become common in the future due to systematic changes in regional climates, hydrological regimes, intensity and duration of high or low flows may be changing as a result of changes in climatic drivers (Figure 2). Numerous severe floods have been reported globally in recent years, for example the July 2021 flood in various European countries causing more than 200 fatalities or the floodings in the same year in Northern China that affected more than 1.76 million people. Hence, there is growing concern that high flow events will become more frequent due to climate change. Some studies have argued that the observed changes in climate (e.g., increases in precipitation intensity) are already influencing river floods (Kundzewicz et al., 2007).

As the atmosphere is getting warmer (IPCC, 2021), it can hold more water vapor, leading to an increasing potential for intense precipitation. It is still unclear how the increase of the frequency and intensity of rainfall events will increase flood risk as changes in river flows often result from non-linear interactions between changing precipitation and evapotranspiration, and basin properties (Arnell, 2011; Laizé and Hannah, 2010). Increased evapotranspiration due to higher global temperatures may shift the

fraction of precipitation that runs off as surface water or infiltrates to the subsurface as recharge (Condon et al, 2020).

Another question arises when discussing possible impacts of climate change on river flow: what are the likely effects of a changing hydrological cycle on flood magnitudes?

Empirical studies from North America and Europe found no evidence of an increase in flood frequency or magnitude during the 20th century, although increases in low to moderate streamflows have been widely reported. Published literature indicates that sensitivity of the mean streamflow to precipitation is much greater than that of peak streamflow, and that precipitation sensitivity decreases as flood return period increases. Therefore, while flood peaks are quite likely to increase if precipitation increases, their fractional change relative to a given fractional change in the mean precipitation is less than the fractional increase in the mean flow (Lins, 2006).

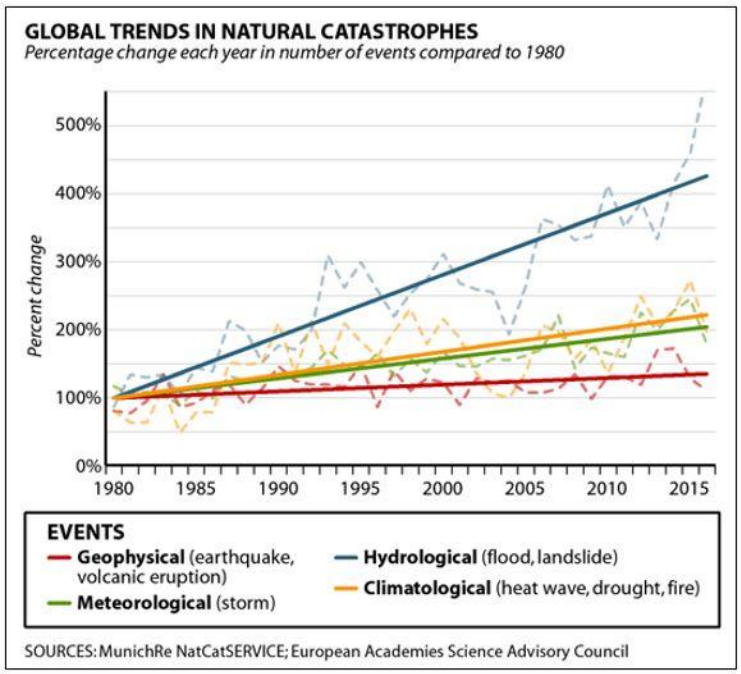

Figure 2 : Trends in natural catastrophes between 1980 and 2015

On a more practical level, much of flood planning and management is based on empirical approaches to assess flood risk such as simple extrapolations from observations to estimate extremes. However, with challenges related to changes in both landscapes and climate, it is argued that a better understanding of flood-driving processes is required for better projections of future flood risk (Blöschl, 2015). Many studies (Marsh, 2008; Schröter et al, 2015; Blöschl, 2013) have investigated root causes and key drivers of extreme floods events in specific sites. Such efforts can provide new insights for large-scale flood hazard assessment and additional knowledge required for planning scenarios for national disaster response and spatial risk assessment. Flood generating mechanisms will be further discussed in the next section.

C. River flood generating mechanisms

Most major floods are characterized by a synergistic combination of atmospheric causes and antecedent basin properties that condition the climate-runoff relationship (Hirschboeck, 1991). As a result, process-based causes of floods are usually classified into three categories based on the hydro-climatology, the hydrology of a catchment and the hydrograph generated during a flood event (Tarasova, 2019). The following section addresses the first two as the latter does not focus on the generating mechanisms of floods or high flow events.

1. Atmospheric circulation and precipitation

Precipitation timing and spatial distribution associated with catchment properties are important factors in whether floods occur or not. To understand the origin of meteorological floods, the temporal and spatial scales of atmospheric processes leading to floods should be considered in conjunction with the temporal and spatial scales of hydrological aspects related to catchments. For this purpose, flood hydro-climatology can provide a framework to better understand atmospheric causes of flooding (Hirschboeck,1988). Flood generating atmospheric phenomena differ in both time and spatial scale; larger scale precipitation processes (macro-scale and synoptic scale) such as extratropical cyclones are associated to moderate to heavy rainfalls over fairly large regions, leading to floods that develop over tens of hours to days and affect large geographic regions (Wohl, 2000). Mesoscale or storm scale phenomenon such as tropical storms or convective thunderstorms are linked to rapid runoff and extreme flash flooding in more localized regions.

In contrast to this hydroclimatic approach that focuses on weather systems and lifting mechanisms, other approaches classify floods according to atmospheric circulation patterns, cyclone tracks and moisture transport. Hirschboeck (1988) hypothesized that exceptional floods in basis of all sizes could be related to anomalies in the 30 large scale atmospheric circulation. This method has been applied to determine moisture transport pathways associated with floods in the United States (Hirschboeck, 1988).

In the European scale, the most common atmospheric predictor of high flows is the circulation type (Hannah et al, 2014). Prudhomme and Genevier (2011) demonstrated that at the river basin scale, some circulation patterns occur more frequently before and during a flood than in any other period and therefore, showed the potential of using atmospheric field patterns e.g., mean sea level pressure to provide information on flood occurrence. Other studies have focused on the link between large-scale climate indices like the North-Atlantic Oscillation Index, defined as the sea level pressure difference between a site in the Azores and an Icelandic station and have shown that it is significantly correlated with stream flows in Europe. A negative NAO is associated with a lower than usual streamflow in northernmost Europe, and a higher-than-normal streamflow in most of the rest of Europe. This is mainly related to a southward displacement of winter storms and moisture transport into Southern Europe (Dettinger et Diaz, 2000). A positive NAO is linked to a northward displacement of storms and moisture and to higher stream flows in northernmost Europe as shown in figure 3.

It should also be pointed out that large-scale indices (i.e., NAO) can mask more specific and seasonal climate dynamics but can be informative in long-term studies (Hannah et al, 2014). Moreover, directly relating atmospheric conditions to flood causality can be a complex matter as some regional responses to teleconnections (i.e., El Niño–Southern Oscillation) can be detectable in precipitation records and not in flood records, as they can operate on much longer climatic scales (Hirschboeck, 1991).

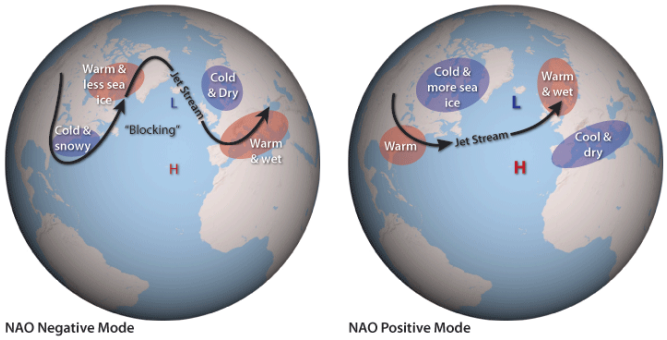

Figure 3 : Influence of pressure patterns on the strength and location of the jet stream and the path of storms across the North Atlantic (from: Climate.gov)

2. Other meteorological and antecedent land-surface conditions

Existing literature has demonstrated that future changes in streamflow extremes are unlikely to be driven by precipitation alone (Sharma et al, 2018). Other conditions related to the catchment such as antecedent wetness, air temperature through snow melt, basin size can also modulate the flood response. Ivancic and Shaw (2015) suggest that any evaluation of precipitation intended to inform discharge should condition precipitation by concurrent watershed moisture status. The following section addresses the mechanisms behind the role of antecedent land-surface conditions on river flow extremes.

2.1. Soil moisture and subsurface water

Soil moisture storage can influence the catchment response to a precipitation event. A large soil infiltration capacity can limit surface runoff. However, once a soil becomes saturated, precipitation can quickly lead to runoff. Evapotranspiration can also modulate the soil response to a precipitation event by conditioning the soil water storage, especially during the summer. Soil moisture also controls potential streamflow generating processes that could lead to floods:

- Hortonian overland flow

This process occurs when rainfall intensity exceeds the soils infiltration capacity or when rainfall is particularly intense. It is considered as the principal generation mechanism for flash floods in arid and semi-arid regions (Davie, 2019).

- Subsurface storm flow

Subsurface storm flow occurs during storm events when water infiltrates very quickly and moves laterally through the soil to enter the stream channel (Dunne, 1983).

- Saturation overland flow

This process is associated with saturated soils or regions with shallow groundwater tables. It can also occur after a lengthy episode of antecedent precipitation or at the end of snowmelt season when soil moisture is at a maximum (Hirschboeck, 1991).

2.2. Snow and snow melt

Snow cover and snow melt occurs in colder regions where precipitation can fall in the snow, during the winter. As temperatures increase later in the season, the stored snow cover can be released during spring. This can lead to a more saturated soil, which can possibly cause higher surface runoff. The presence of frozen ground in the winter can also prevent infiltration and enhance a flood response. Some snowmelt-related floods can also occur when rain falls on an antecedent snow cover (Wohl, 2000). This process depends on the size of the existing snow pack and the falling rain's temperature, as a smaller snow pack will tend to absorb the rainfall and not produce snowmelt. Warmer rainfall tends to increase snowmelt. Moreover, snow-melt induced floods is linked to warmer and prolonged rainfall events.

2.3. Catchment attributes

Stein et al (2021) investigated the influence of climate and catchment attributes (i.e., slope, area, shape, soils and vegetation) on flood generating processes in catchments from the United States and has demonstrated that climatic attributes such as fraction of snow, aridity and mean precipitation have the strongest influence. The importance of catchment attributes has been shown to vary according to flood generating processes and climates. Moreover, catchment characteristics such as basin area, slope and shape were not shown to be influential on flood processes (i.e., snow/rain floods, snowmelt floods, excess rain floods etc.).

3. Multicausality of flood generating processes

Individual flood events can be caused by multiple mechanisms (Merz and Blöschl, 2003). Therefore, it is important to understand the role of the combination of flood-generating factors. For example, the June 2013 flood in the Upper Danube was mainly caused by high antecedent soil moisture combined with a temporal shift of flood peaks at the confluence of the Bavarian Danube and the Inn, and rainfall blocks which resulted in a large flood wave (Blöschl et al, 2013). This demonstrates the links between atmospheric and climatic mechanisms and catchment and river processes in generating floods (Merz et al, 2021).

D. Flood typology in Western Europe

The following section provides a brief insight on flood types in some European countries where nation-wide causative classifications have been established.

1. Czech Republic

Floods in the Czech Republic have been classified into the following categories (Brázdil et al., 2006) in terms of their generating causes:

- rain-generated floods caused by liquid precipitation, either from continuous precipitation or from torrential rains;
- snowmelt floods due to the sudden melting of snow cover at positive temperatures in the winter and spring seasons;
- mixed floods resulting from a combination of snowmelt and rain;
- ice-jam floods when sudden warming may cause ice to move and block the discharge profile by accumulation.

2. Germany

Beurton and Thieken (2009) analyzed the seasonal distribution of annual maximum floods in various gauging stations in Germany and have identified using a cluster analysis three regions:

- Cluster A: catchments in the western and central part of Germany where floods are influenced by the Atlantic climate and by westerly precipitation fields. Floods typically occur in the winter.

- Cluster B: catchments in the north and eastern part of Germany with a similar flood regime to cluster A, but shifted towards the spring due to the continental influence. Intense summer rainfall can lead to extreme floods.

- Cluster C: the cluster covers the Alps and pre-Alps and shows a summer flood regime due to the low temperature which maintains the snowpack and leads to snowmelt during spring or summer.

3. United-Kingdom

Frontal rainfall is the most dominant cause of flooding in the United Kingdom due to its temperate and maritime climate. Larger catchments respond more to prolonged rainfall over many days. Intense rainfall also contributes to pluvial flooding.

Flood events due to snowmelt are far less frequent than rainfall-related events, especially since the 1980s when snowfall became less frequent.
Because runoff exhibits a strong seasonal cycle driven by evaporation, the main flood season occurs in the winter and fall, when the evaporation is not very significant (Hannaford and Hall, 2012).

4. Flood seasonality in Western Europe

Hall and Blöschl (2018) identified spatially distinct regions with characteristic patterns of temporal flood occurrence in Europe. A transition in the pattern of mean seasonality is apparent, from winter floods in western Europe to late spring and early summer floods in eastern Europe has been demonstrated. A large-scale cluster analysis shows that in Western, Central and Southern Europe, the primary flood season is between December and March. For mountainous regions, the primary flood season is between May and August. In Central and Eastern Europe, floods mostly occur between February and April. Analyzing seasonality of flood events can help flood process understanding and predict possible shifts in flood regimes due to changes in climate.

5. Flood drivers in Europe

Various methods have been used in large-scale studies to assess flood generating processes in Europe. A first approach related changes in flood timing to changes of considered drivers in order to infer the generating processes (Blöschl et al., 2017, 2019).
Berghuijs (2019) used circular statistics to attribute to each catchment the flood driving mechanism by comparing the average timing of floods with the timing of potential flood drivers. Both approaches use only average timing for both floods and flood drivers and do not identify processes for individual events.
Stein (2019) developed a methodology to identify both the dominant flood generating process and single-event generating processes in catchments using only the timing of annual maximum flow.
Existing studies have yet to use actual streamflow measurements to infer flood drivers. Moreover, annual maximum flow is often used as in indicator of the occurrence of a flood, rather than a flood with physical senses e.g., when the river leaves its banks and spreads out onto the floodplain.
In terms of flood generating processes, heavy rainfall with high antecedent soil moisture has been identified as the dominant driver of floods in Europe (Berghuijs, 2019). Similarly, flood changes in some parts of Europe were found to be closely associated with changes in both precipitation and soil moisture (Blöschl et al, 2019). Stein et al (2019) also identified excess rainfall (rain on wet soils) as the dominant driver in most parts of Europe.
With regards to underrepresented aspects in causative classification of flood events, Tarasova (2019) identified the role of spatiotemporal characteristics of rainfall as a possible indicator that could provide additional insight on processes.

E. Thesis objectives and outline

The general objectives of this thesis are to study the importance of potential river flood generating processes over a wide range of near-natural catchments in Europe and to determine dominant processes in different spatiotemporal scales. To achieve these objectives, use is made of a European runoff dataset to characterize floods and both observational and modeled datasets for considered drivers. An explicit analysis of the linkage between peak runoff and drivers is done over different time scales. The relevance of each driver is analyzed though correlations with flood peak magnitudes.

Previous studies have almost exclusively focused on rainfall, soil moisture and snow melt as potential flood drivers for the continental assessment of flood generating mechanisms. The goal of this study is to extend the range of considered drivers and to investigate the potential variations of their relevance with respect to considered flood time scale. The results can provide new insights in the understanding of regional differences in time-scale-differentiated process controls of floods.

II. Materials and methods

A. Data

1. Streamflow data

Long-term (1984-2007; 24 years) daily flows were obtained for 436 catchments (Table 1, Figure 4) from the UNESCO's European Water Archive (EWA), a reference dataset of near-natural streamflow (Stahl et al, 2010). EWA contains river flow records from over 4,000 monitoring stations across 30 countries (Figure 5). Originally hosted by the Center for Ecology and Hydrology in the UK, its maintenance was passed to the Global Runoff Data Centre at the Federal Institute of Hydrology in Germany in 2004. Data archived in the EWA is supplied on a voluntary basis by hydrometric agencies across Europe and is freely available. This dataset is also used in the European Flood Database (Hall et al, 2015) which comprises of annual maximum and daily mean discharge series, from over 7000 hydrometric stations of various data series lengths.

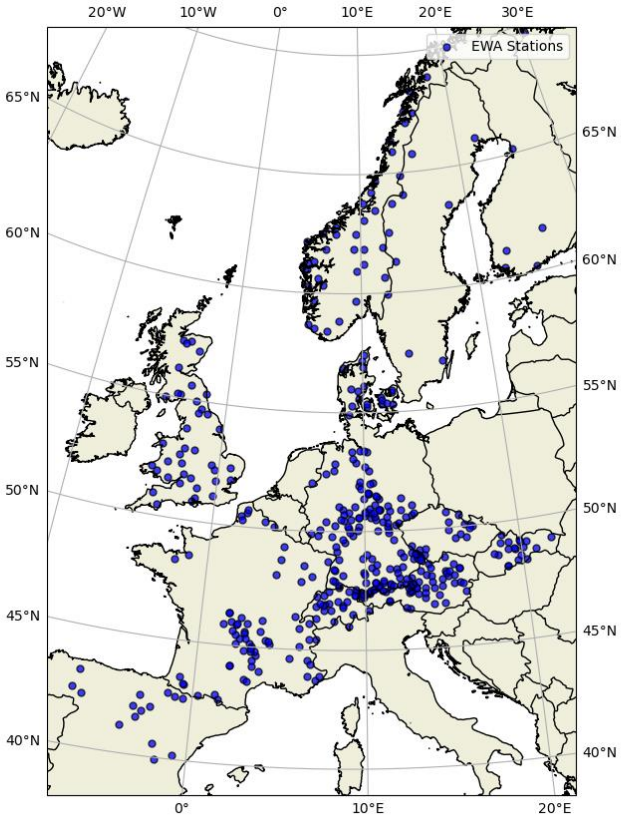

Figure 4 : European Water Archive stations

The EWA dataset has been used for many international studies on: the variability over time in European annual and seasonal river runoff (Arnell,1994), classification of river flow regimes in Europe (Krasovskaia et al., 1994), the link between river flow and the North Atlantic Oscillation (Shorthouse and Arnell, 1997, 1999), streamflow trends in Europe (Stahl et al, 2010). Although the data collected

corresponds to homogenous, quality-controlled records of daily mean flow, two more quality checks were done following the recommendations in Gudmundsson et al (2018):

1. Days for which Q<0 are flagged as suspect, where Q denotes a daily streamflow value.
2. Daily values with more than 10 consecutive equal values larger than zero are flagged as suspect. This rule is motivated by the fact that many days with consecutive streamflow values often occur due to instrument failure.

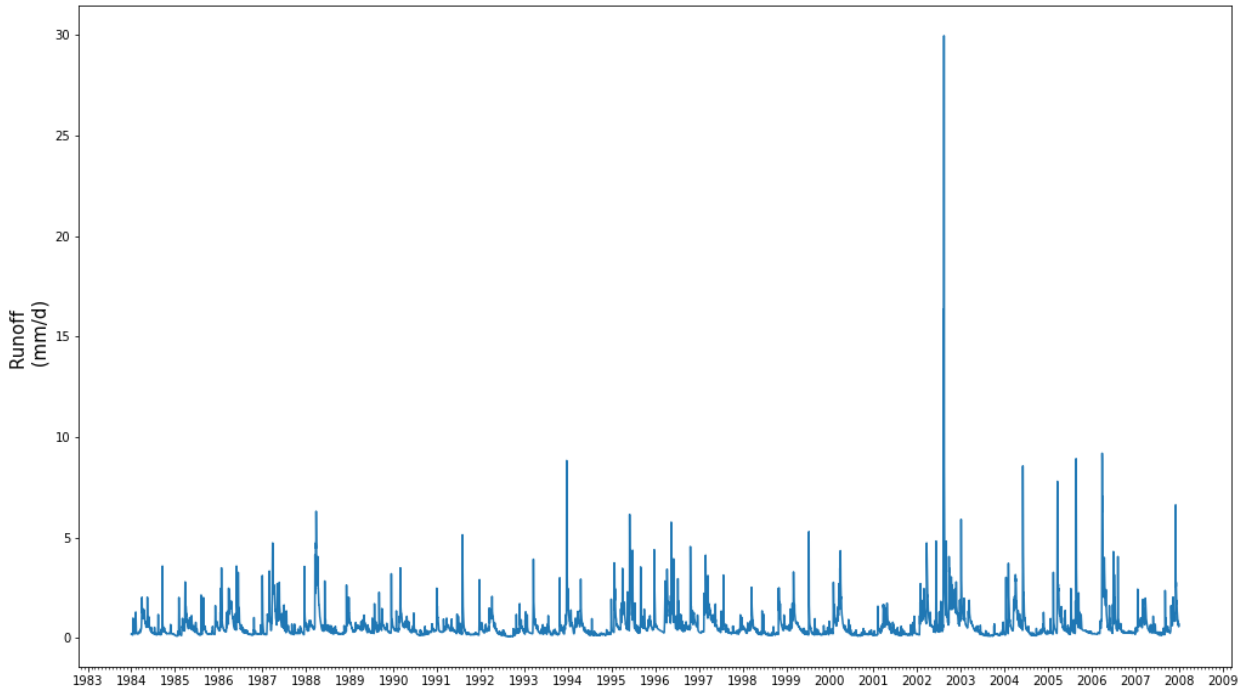

Figure 5 : Daily streamflow records in the Volyňka catchment (Czech Republic)

The number of stations from each country varies from one or a few (e.g., the Netherlands and Finland) to over 140 (e.g., Germany). Table 1 provides a corresponding summary.

Table 1: Details of the EWA stations

Country	**Number of stations**	**Mean catchment area (km ^{2})**
Austria	47	206
Switzerland	23	164
Czech Republic	14	288
Germany	137	291
Denmark	19	267
Spain	15	452
Finland	5	2059
France	68	754
Netherlands	1	351
Norway	40	416
Sweden	9	1194
Slovakia	19	230
United Kingdom	30	382
Total	436	

2. Potential drivers' data

The following section presents the data used in the study (Table 2) to estimate potential high flow drivers. Section 3 of the Methodology details the motivation for the selection each potential driver's selection.

Table 2 : Overview of data used to estimate potential drivers

Variable	Type	Unit	Temporal resolution	Spatial resolution	Dataset	References
Rainfall	Observational	mm	Daily	0.25°×0.25°	E-Obs gridded data (v.20)	Cornes et al (2018)
Air temperature	Observational	°C	Daily			
Evapotranspiration	Model-based	mm	Daily		Global Land Evaporation Amsterdam Model (v3.5a)	Martens et al (2016)
Snow-melt	Model-based	mm	Daily		Simple Water Balance Model	Orth and Senevirtane (2015)
Soil moisture	Reanalysis	$m^3 .m^{-3}$	Daily		European ReAnalysis 5 (ERA-5)	Copernicus Climate Change Service (2017)
Leaf Area Index	Observational	Dimensionless	Monthly	0.5° x 0.5°	GEOV2-AVHRR	CNES-Theia
North-Atlantic Oscillation Index	Observational	Dimensionless	Daily	-	NOAA's National Weather Service	Dool et al , 2000

E-Obs is a gauge-interpolated daily gridded observational dataset over Europe. Rainfall data corresponds to the total daily amount of rain, snow and hail measured as the height of the equivalent liquid water in a square meter. Air temperature is the mean temperature measured near the surface at height of 2 meters (Figure 6).
The Global Land Evaporation Amsterdam Model (GLEAM) is a set of algorithms that separately estimate the different components of land evaporation: transpiration, bare-soil evaporation, interception loss, open-water evaporation and sublimation. Evapotranspiration corresponds to the "Actual-Evaporation" (E) product of the GLEAM dataset.

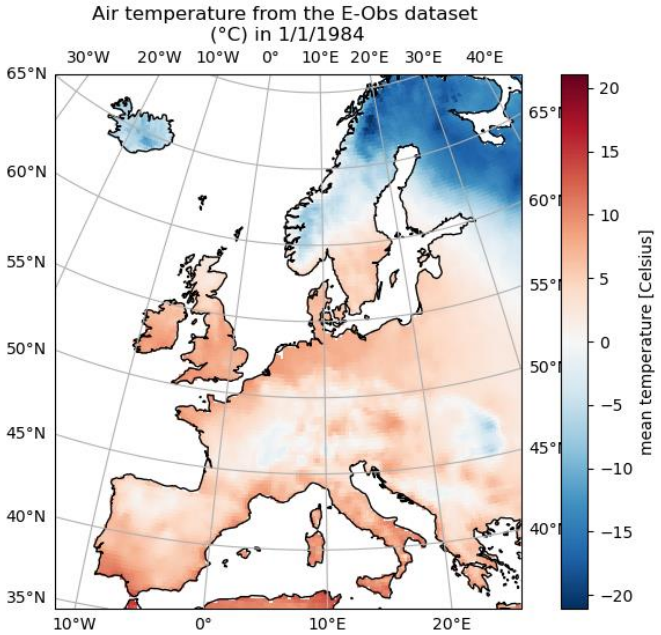

Figure 6 : Daily air temperature (°C) in the E-obs dataset

Daily snow melt is obtained using the Simple Water Balance Model (Orth and Seneviratne, 2015). The model uses a degree-day approach to estimate snow water equivalent, and has been validated against ground measurements (Orth and Seneviratne 2013).
The model is forced with net solar radiation from the ERA-5 dataset and precipitation and air temperature from the E-Obs datasets in the 436 catchments, over the entire considered period (1984-2007). The model includes six calibration parameters, water-holding capacity, runoff and evapotranspiration ratio exponents, a maximum evaporative fraction, a melting parameter for snowmelt and an inverse streamflow recession timescale parameter. Selected parameters correspond to the best-performing parameter set provided by Fallah et al (2020). Nash-Sutcliffe Efficiency values are shown in the Appendix (A.2.) for each catchment. Outputs of the model include precipitation that falls in form of snow. Snow melt is then inferred from the daily difference in accumulated snow.
Soil moisture corresponds to volumetric soil water in three different layers:

- Layer 1: 0 - 7cm
- Layer 2: 7 - 28cm
- Layer 3: 28 - 100cm

It is provided by the ERA5 dataset, the fifth generation ECMWF atmospheric reanalysis of the global climate. Reanalysis is a systematic approach that combines model data with observations from across

the world into a globally complete and consistent dataset. Reanalyses are created via a data assimilation scheme and model(s) which ingest all available observations over a certain period. A limitation of this approach is the spurious variability integrated in the reanalysis output due to biases in both observations and models.

The Leaf Area Index is estimated using satellite observations from the GEOV2 (GEOLAND2 Version 2) - AVHRR (Advanced Very High-Resolution Radiometer) product provided by the THEIA Land Project.

Given that all data is gridded (except for the North Atlantic Oscillation Index) and in order to attribute specific values to the selected catchments, a "nearest neighbor" method is used to assign the nearest grid to the grid in which the catchment is located as shown in figure 7 for precipitation data. All data is gathered for each catchment as shown in figure 8.

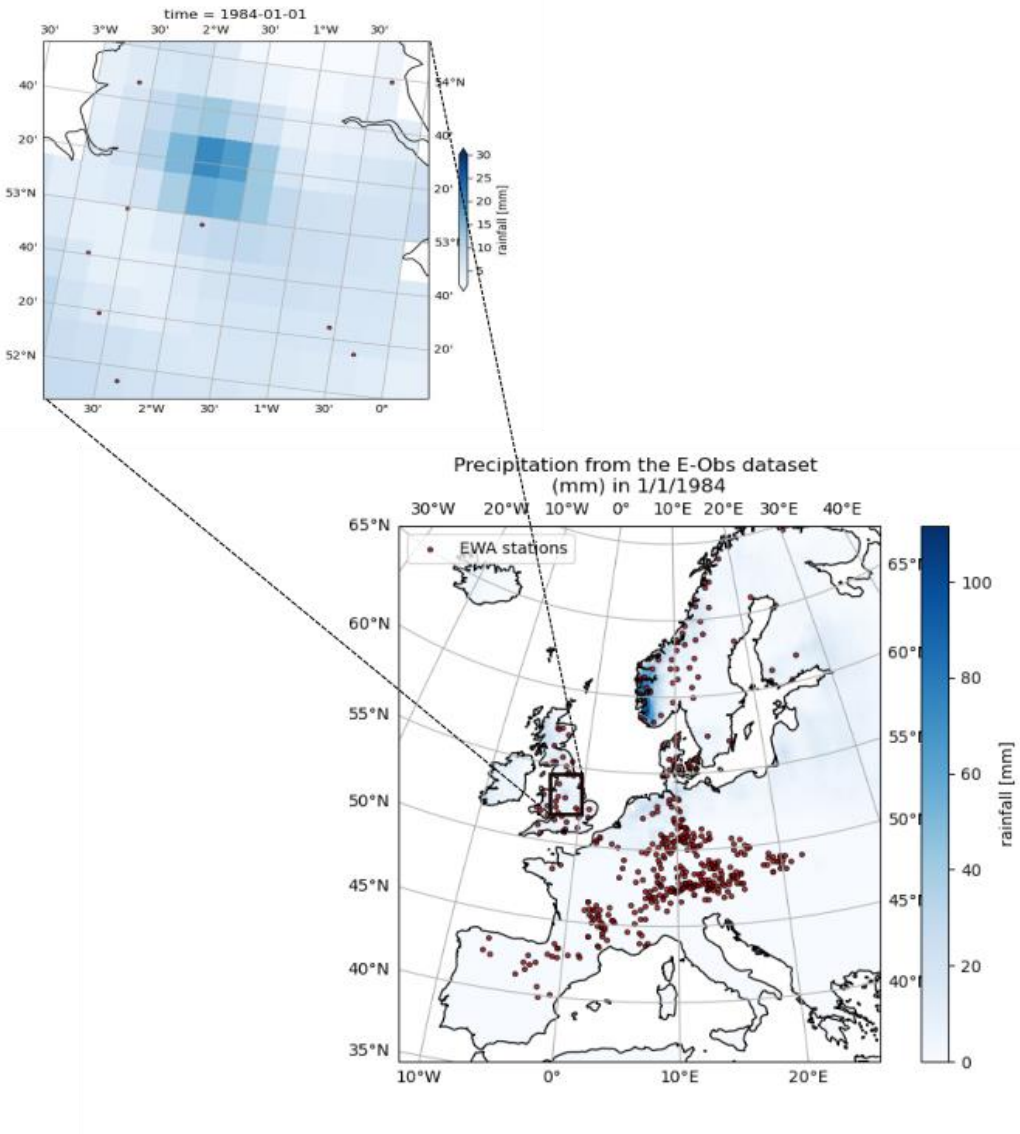

Figure 7 : Flood driver's data collection for the catchments

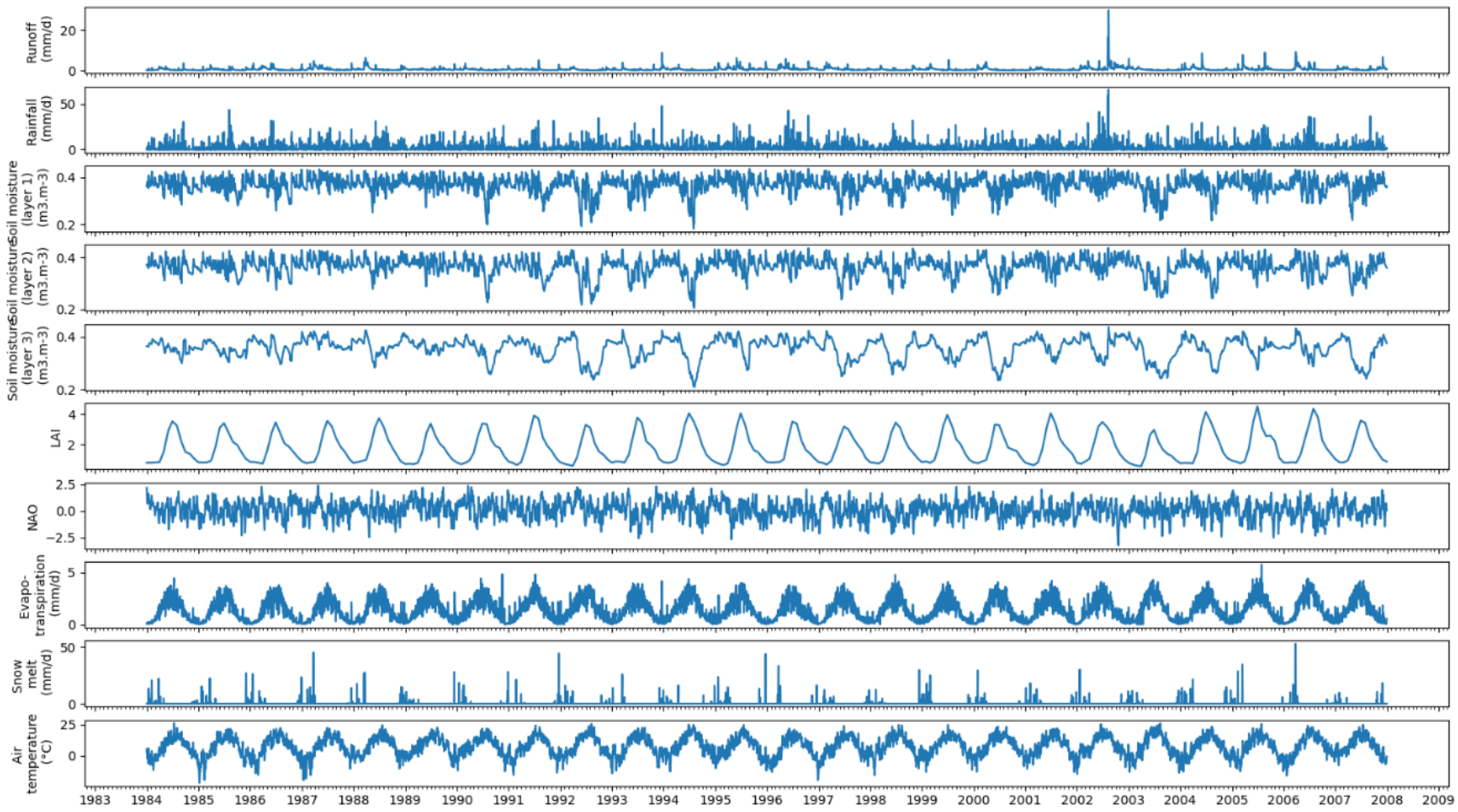

Figure 8 : Runoff and potential high flow drivers in the Volyňka catchment (Czech Republic)

B. Methodology

1. Catchment selection

Before selecting flood events from daily streamflow records and to ensure data consistency in the time period of the study (1984-2007), catchments with more than half of one year of missing data are excluded (Figure 9). 275 catchments are then considered to have valid runoff data.
As the study focuses primarily on near-natural catchments with no or minor disturbance due to human influence on river flow, only a subset of catchments in which a simple conceptual hydrological model e.g., Simple Water Balance Model (from Orth and Seneviratne, 2015) exhibits satisfactory performance. From the 275 catchments, only catchments that had a score of NSE higher than 0.36 were selected. The NSE criterion is adopted from O et al, 2020. As a result, only 174 catchments from 8 countries had a score of NSE higher than 0.36 (Figure 10). The median basin size is 273 km^2, ranging from 7 to 2340 km^2. 2 catchments were excluded due to missing Leaf Area Index data. Details of individual catchments are shown in the Appendix (A.1.). Nash-Sutcliffe Efficiency values are provided in the Appendix (A.2.).

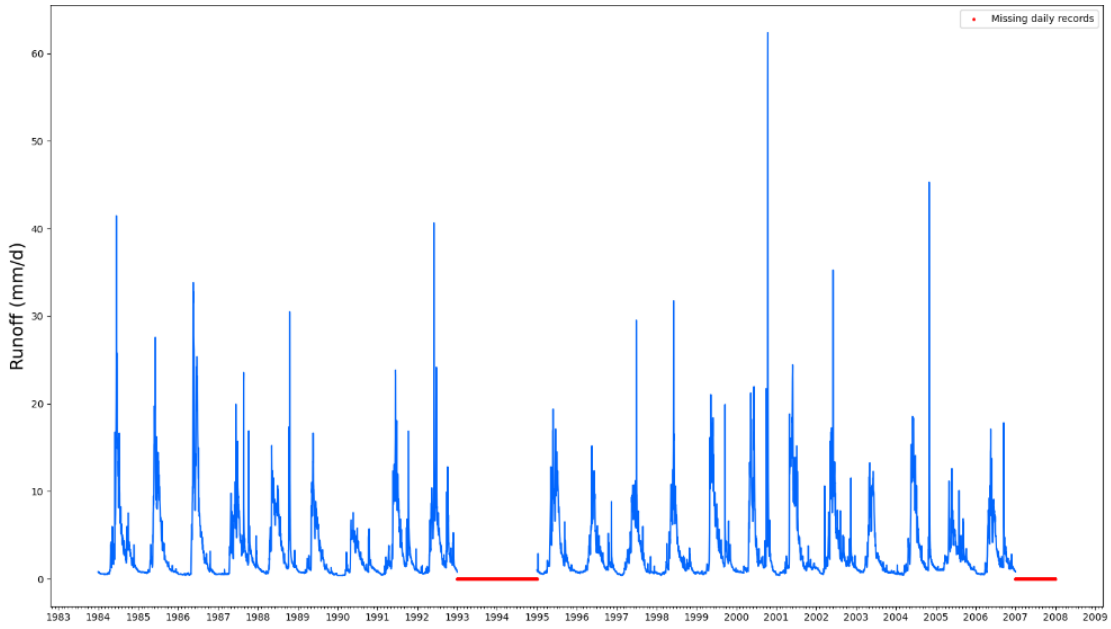

Figure 9 : Daily streamflow record in the Krummbach catchment (Switzerland)

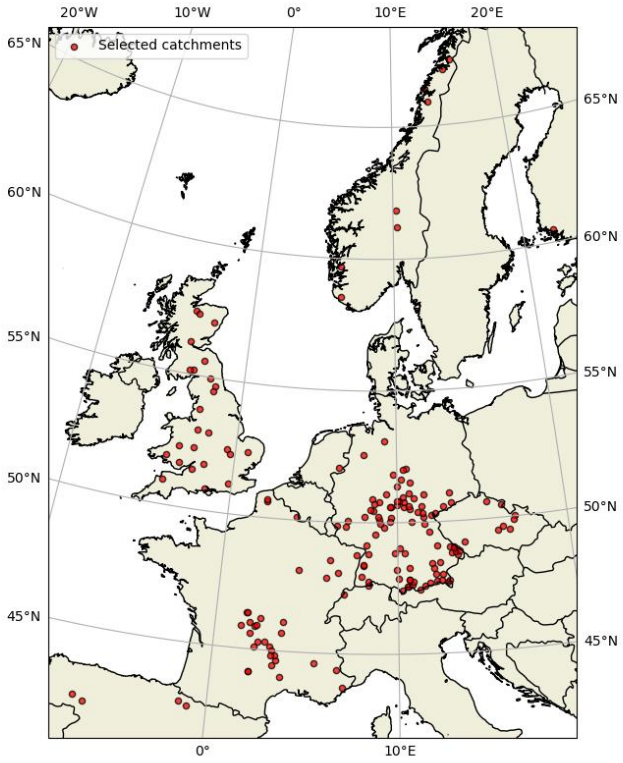

Figure 10 : Selected catchments from the European Water Archive

2. Identification of high flow events

According to the WMO/UNESCO definition of "flood" in the "International Glossary of Hydrology" (World Meteorological Organization – WMO, 2012) which is:
"(1) Rise, usually brief, in the water level of a stream or water body to a peak from which the water level recedes at a slower rate.
(2) Relatively high flow as measured by stage height or discharge"., we select flood events from daily streamflow records of each catchments using a series of criteria. First are excluded daily records with an accumulated ten-day rainfall below 3 mm to avoid including possible outliers. We select then monthly maxima from which the 30 highest peaks per season (see section 4 of the Methodology) are selected. To ensure that peaks correspond to independent flood events, we only select peaks separated by a three-month time window. Finally, we select the 10 highest runoff peaks per catchment and per season. By applying the aforementioned criteria, we define floods as high flow events, based on the runoff magnitude only, independently of the duration of the event or the shape of flood hydrograph. This method used to identify flood events does not necessarily imply that the river overtops the banks and reaches the floodplain. Figure 11 shows selected flood events in one catchment.

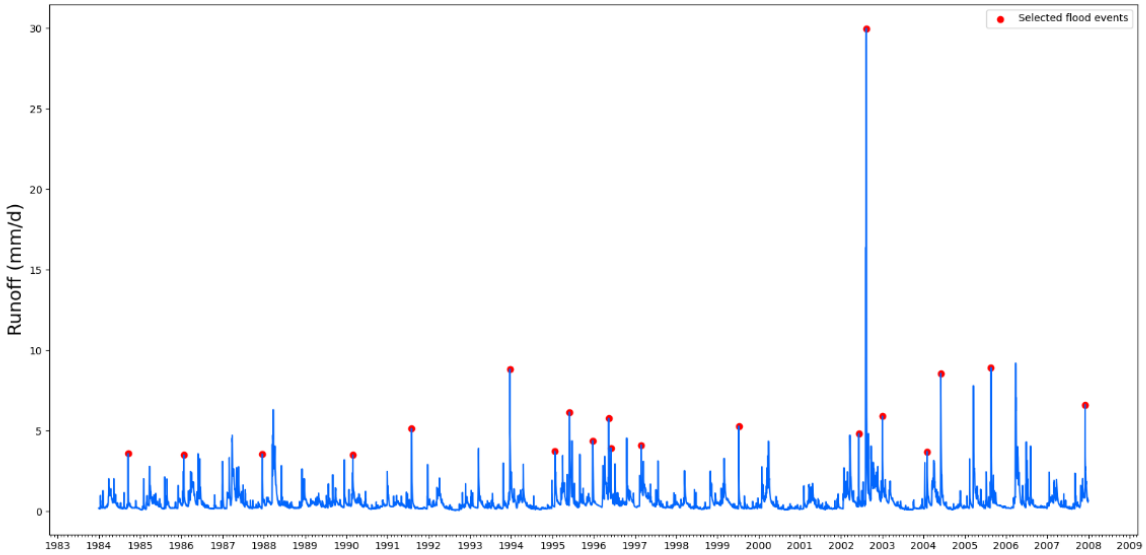

Figure 11 : Selected flood events from daily streamflow records in the Volyňka catchment (Czech Republic)

3. Selection of potential flood drivers

After selecting high flow events, potential drivers are inferred from the parameters gathered in section 2 of Data. Drivers are categorized by the plausible relationship (negative or positive) they could have with runoff. From daily rainfall data, accumulated rainfall preceding a flood event is selected as a potential flood driver. To differentiate between short rainfall events and long rainfall events, which could potentially have a different effect on generated runoff, we also include the ratio between the peak daily rainfall before a flood event and the sum of antecedent rainfall. The ratio is an indicator of the distribution of the rainfall event. A rainfall event that occurs only on one day before a flood event would have a ratio of 1. The ratio ranges between 0 and 1.

Given that floods result from the interaction between precipitation, soil moisture and snow-melt, the last two are also selected as potential drivers of floods. It is assumed that they have a positive relationship with runoff. Air temperature is also selected as a potential driver, and is also a proxy for snow-melt, snow-to-rainfall transition and evapotranspiration in different seasons. As precipitation is partitioned into surface runoff and evapotranspiration, the latter is also selected as a driver and could negatively affect runoff, similarly to the Leaf Area Index which is an indicator of interception. Interception can, in certain conditions, positively affect runoff (e.g., falling water in the soil after strong winds).

As for the North-Atlantic Oscillation index, when it is in a positive phase, northern Europe experiences increased storminess and precipitation, and warmer-than-average temperatures that are associated with the air masses that arrive from lower latitudes, while southern Europe experiences decreased storminess and below-average precipitation. When it is in a negative phase, southern Europe experiences increased storminess, above-average precipitation, and warmer-than-average temperature as opposed to Northern Europe. All drivers correspond to antecedent values that precede a flood event for different time scales before the event. To summarize, selected potential flood drivers are:

- Accumulated rainfall;
- Ratio of the maximum daily rainfall and the accumulated rainfall;
- Snow melt;

- Multi-layer soil moisture (layer 1, 2, 3);
- Evapotranspiration;
- Air temperature;
- Leaf Area Index;
- North-Atlantic Oscillation Index.

To investigate how flood drivers vary across time, average potential drivers are computed in different time scales that precede a flood event e.g., 2, 5, 10 and 20 days.

4. Seasonality analysis

4.1. Anomaly extraction

Given that we are interested in the relationship between runoff and potential drivers in a high flow event, it is necessary to isolate the information from each parameter time series from the information that is simply inherent to the season of the year, in order to get a clearer association between runoff and drivers. When looking at relationships between time series of variables, seasonality can reduce the degrees of freedom as the data will not be independent. This seasonal correlation can result in spurious correlations. Therefore, seasonality is removed with the goal of increasing the degrees of freedom. There are many methods to study and extract seasonality from time series such as Seasonal Adjustment or Deseasonalization where the seasonal component is modeled then subtracted from the observations. We estimate the seasonal component from the mean seasonal cycle of each variable, which is computed by averaging daily observations each year (i.e., the mean seasonal temperature on the 1st of January corresponds to the average of temperature the 1st of January in each individual year between 1984 and 2007). To remove the random variations that can appear in the computed mean season cycle, smoothing of the cycle is applied using a centered moving average including both 5 previous and future values to calculate the average at a given point in time. By removing the seasonal component from observations, we obtain anomalies for both runoff and potential drivers. A positive (or negative) anomaly corresponds to a higher (or lower) value than expected in that time of year. The figure below shows an example of deseasonalization of runoff and air temperature in one catchment.

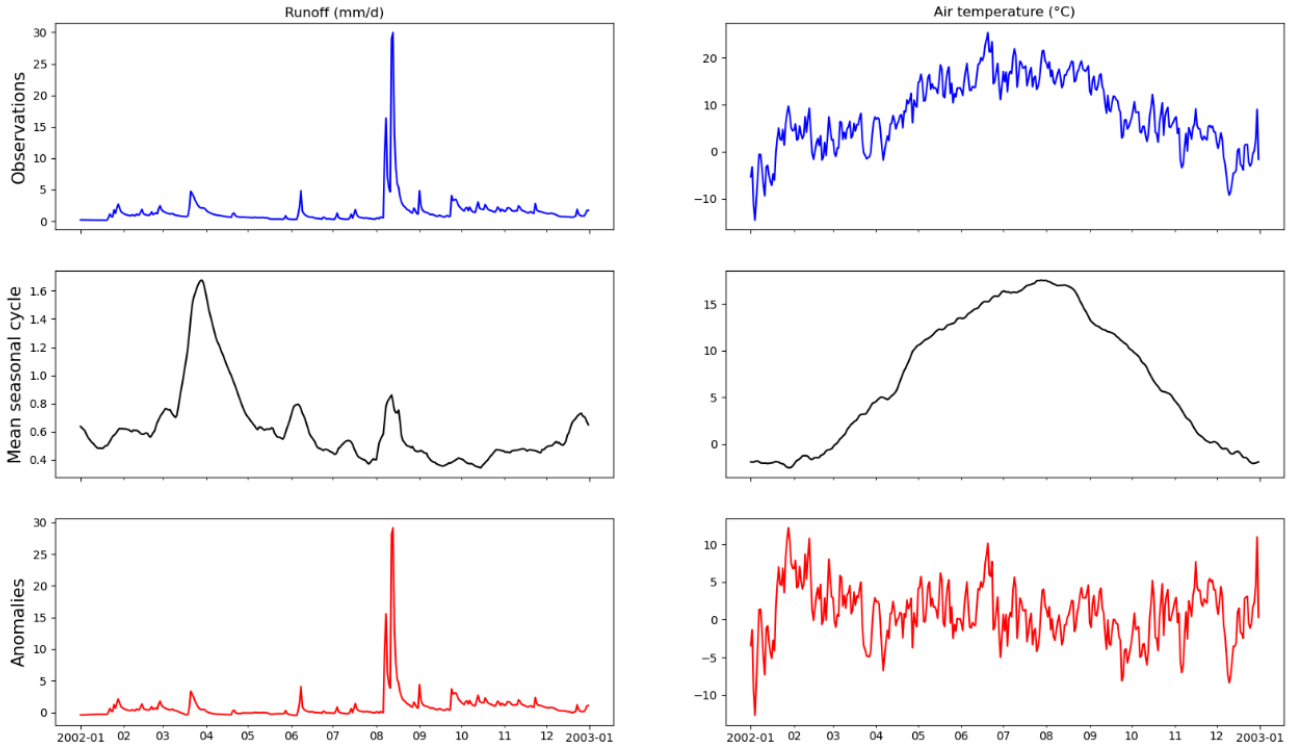

Figure 12 : Deseasonalization of runoff and air temperature in the Volyňka catchment (Czech Republic)

4.2.Seasonality of high flow events

In order to investigate the temporal patterns of flood drivers, we analyze the relationship between runoff and drivers during peak events in various seasons. To avoid possible overlapping flood generating mechanisms in one season, for example spring where floods in the early season could be caused by snow melt and in later by rainfall events, we define a season according to the air temperature: a warm season corresponding to temperatures higher to 10°C where the vegetation is potentially green and active, and a cold temperature with temperatures below 2°C where soil is potentially frozen. This is done by computing the smoothed mean seasonal cycle of air temperature in each catchment and attributing each date of the period between 1984 – 2007 to its corresponding season defined by the mean seasonal cycle, as shown in the figure below.

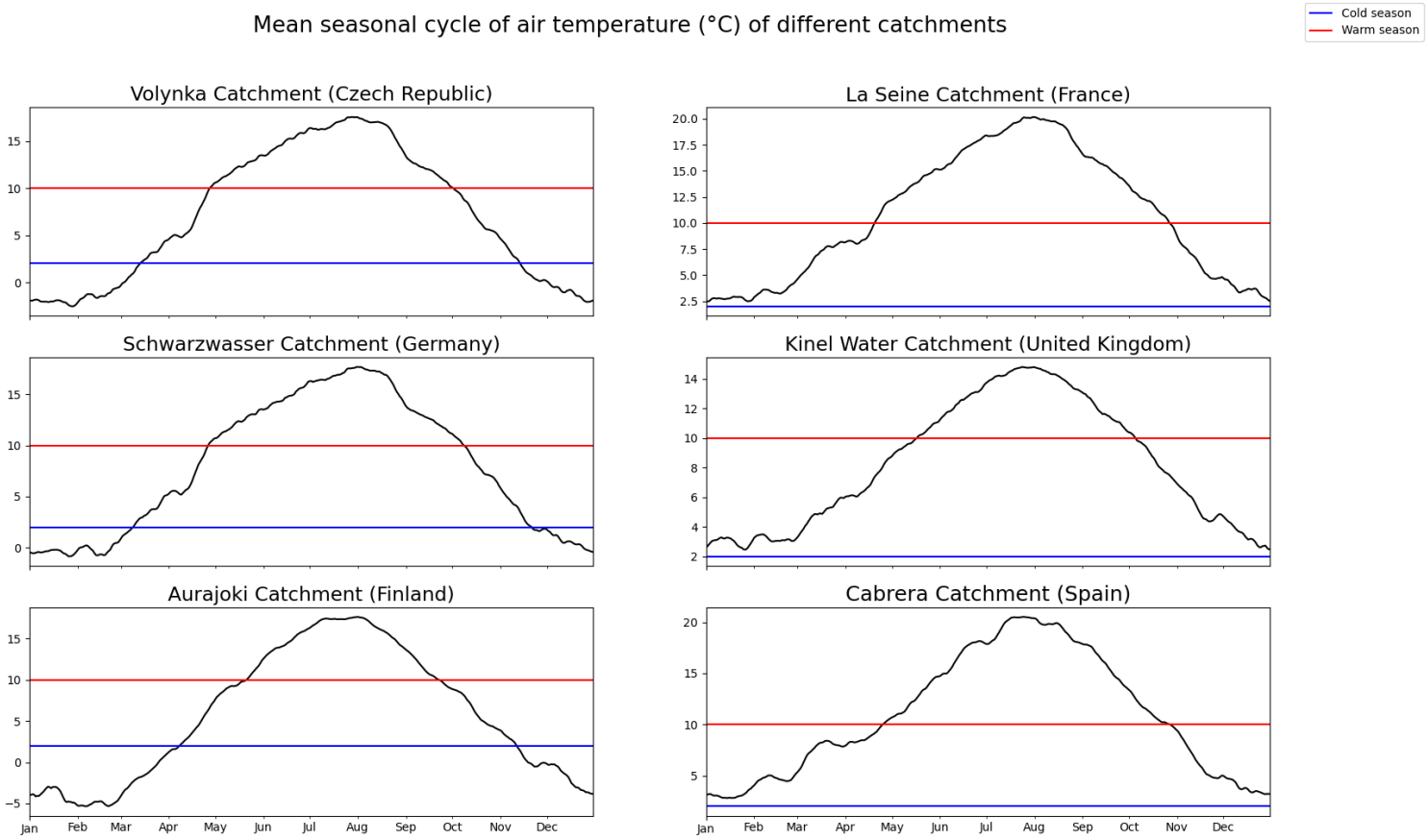

Figure 13 : Mean seasonal cycle of air temperature (°C) of different catchments

5. Correlation analysis

The importance of each driver is assessed using a correlation analysis. Correlation is measured using the Spearman's rank correlation coefficient which, compared to the Pearson correlation coefficient, doesn't assume linearity between variables and is not sensitive to outliers. For each potential driver and for each selected flood event, each pair of driver value and the corresponding runoff value are given a rank. Computation of the correlation coefficient is based on difference scores between a variable's ranking on the first (variable x: Runoff) and second (variable y: a potential driver) sets of values. The formula for difference scores is D = x – y. As results with negative values cancel out positive values, results are squared for use in the analysis. The formula for calculation of the correlation coefficient is:

$$\rho = 1 - \frac{6 \sum D^2}{N^2 - N}$$

ρ: Spearman's rank coefficient;
D: difference between the ranking on both variables x and y;
N: Number of paired ranked scores

The Spearman's rank coefficient varies between -1 and 1. A positive value indicates a positive relationship and a negative indicates a negative relationship, with numbers closest to either -1 or 1 indicating a stronger relationship. Figure 14 shows an example of a scatter plot of different pairs of values used for the correlation analysis.

6. Summary

A first step in the study was to select catchments that had both valid runoff data and exhibit a near-natural behavior with regards to potential streamflow generating processes. From daily streamflow records, flood events were selected in both the warm and cold season. 10 potential drivers were derived from parameters from differing datasets. To determine the temporal importance of each driver, the average of each potential driver anomaly is computed in different time scales that precede each flood event. The importance of each driver is assessed using a Spearman correlation coefficient.

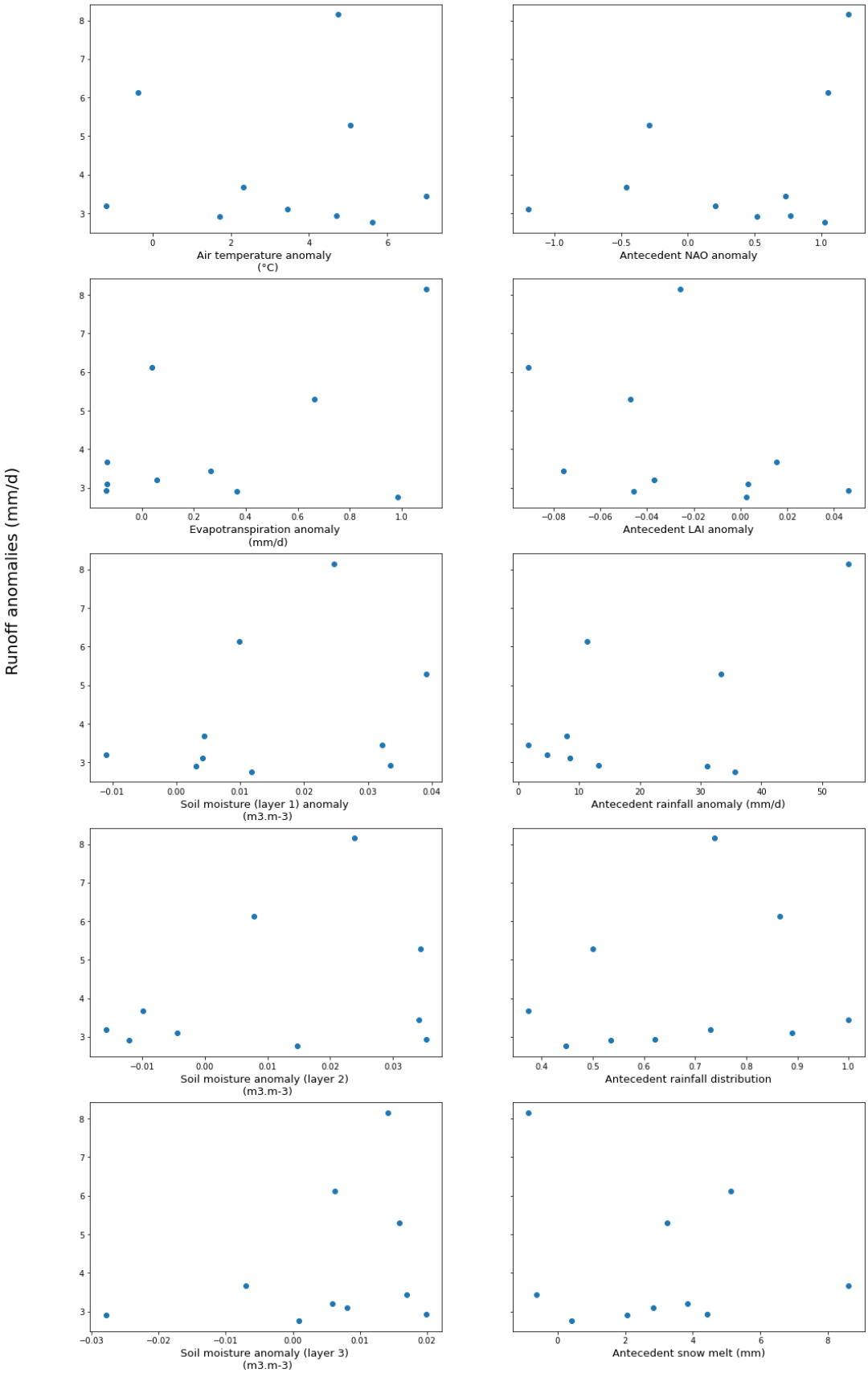

Figure 14 : Scatter plots of runoff versus potential drivers' anomalies five days before a peak event in the cold season (Volyňka catchment)

III. Results

The following section presents the results of the study. This section addresses the dominant flood generating processes identified in both the warm and cold season across different time scales.

A. Dominant flood generating processes

1. During the warm season

The figures below show the dominant flood driver for each catchment in the warm season. Each driver shown corresponds to the parameter with the highest Spearman correlation with runoff anomalies during high flow events. Correlations for the time scale of two days can be found in the Appendix (A.3.)

The figure above displays a diverse set of spatial patterns in flood generating mechanisms.

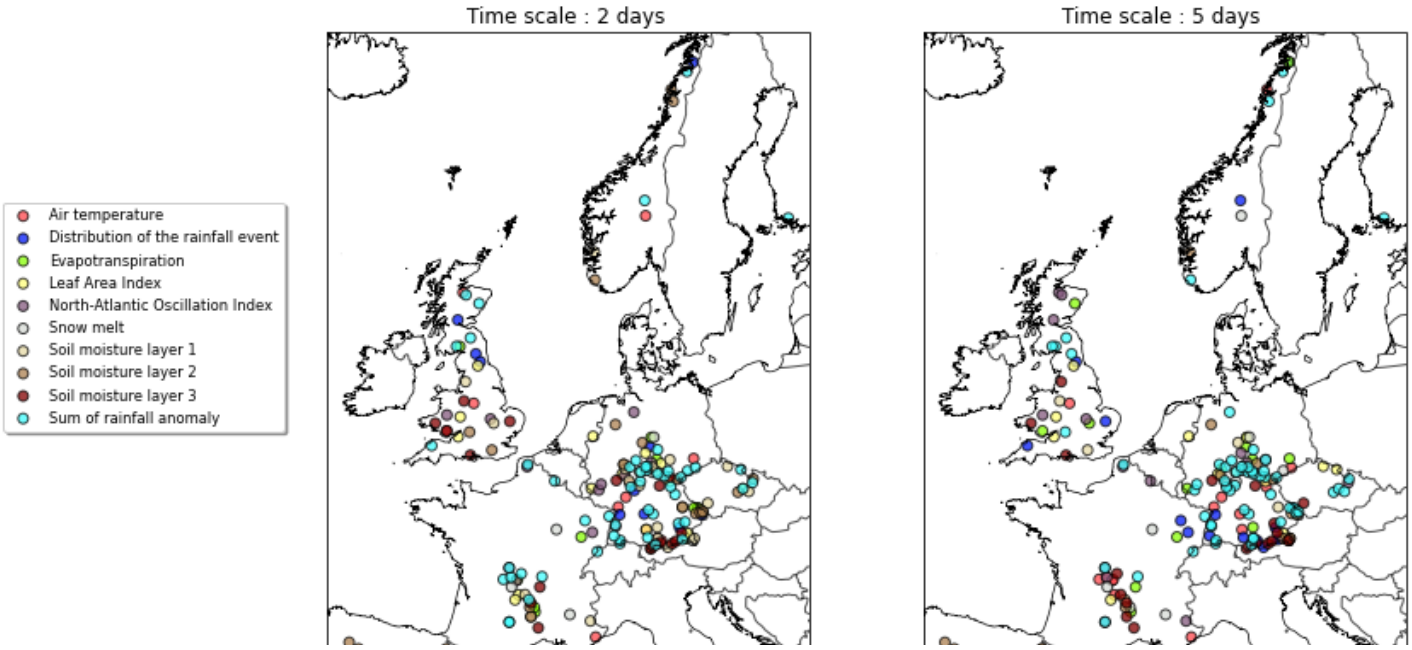

Figure 15 : Dominant flood drivers in the warm season for time scales of two to five days

Except for the center of Germany, a cluster of one flood driver cannot be identified.
The results show that accumulated antecedent rainfall is the most dominant driver in most catchments (for 53 and 57 catchments in time scales of 2 and 5 days). These catchments are primarily located in France and Germany. Soil moisture (layer 1, layer 2 from the ERA5 dataset) is an important driver in catchments located in northern Spain, Czech Republic, the United Kingdom and Germany. Its importance decreases with time, where for example in Germany, the number of catchments where it is an important driver goes from fourteen to four. Soil moisture (layer 3) becomes more relevant between the 2 and 5 days that precede the flood events and is an important driver of 19 catchments, in the center of France and the regions nearing the Alps.

Snow melt is an important driver in a few catchments located in Germany and France (i.e., Saalach, La Vézère) only. The Leaf Area Index is also a relevant driver in some regions in the United Kingdom and Germany.

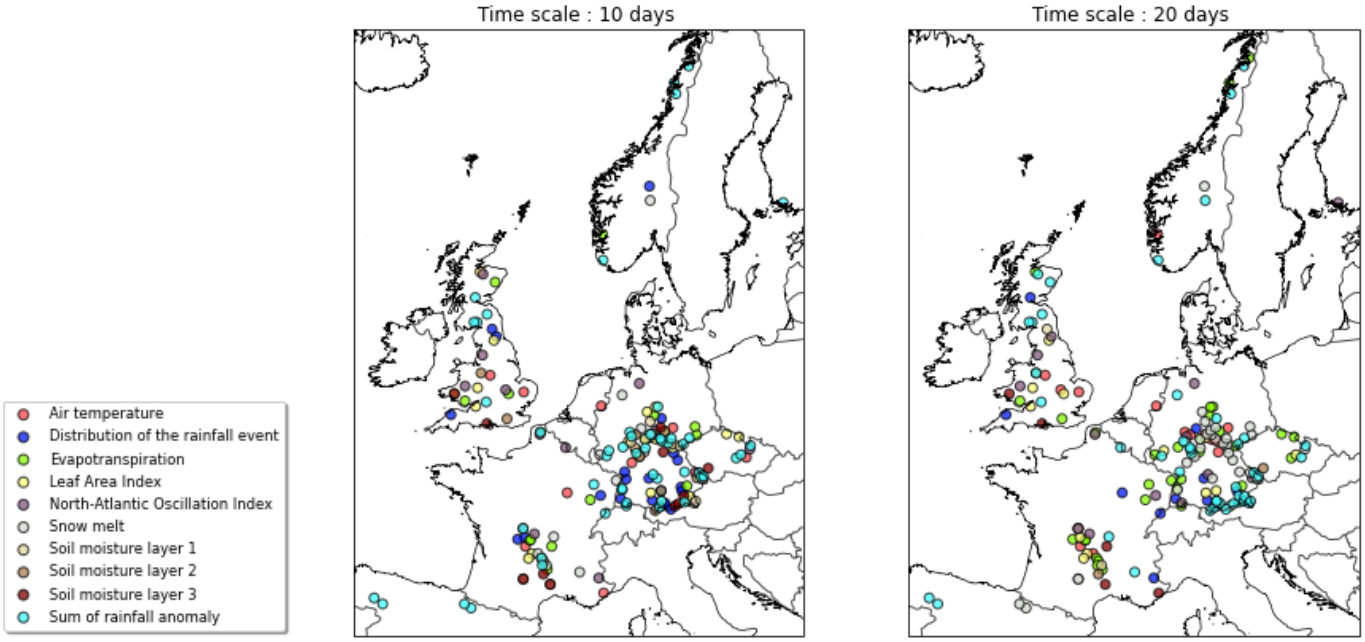

Figure 16 : Dominant flood drivers in the warm season for time scales of ten to twenty days

In the 10 and 20 days that precede a flood event, drivers like evapotranspiration and snow melt become dominant drivers in some catchments. In the warm season, snow melt formed within the 20 days that precede a high flow event is a driver in 26 catchments in the center of Germany. The distribution of the rainfall event plays a stronger role in the time scale of ten days. The table below summarizes the drivers and the number of catchments and their respective dominant driver. The focus is only on the five most dominant driver.

Table 3 : Number of catchments and their associated flood generating mechanism in the warm season

Time scale (days)	2		5		10		20	
Drivers	Accumulated rainfall	53	Accumulated rainfall	57	Accumulated rainfall	51	Accumulated rainfall	44
	Soil moisture (layer 1)	23	Soil moisture (layer 3)	19	Distribution of the rainfall event	21	Evapotranspiration	32
	Soil moisture (layer 2)	21	North-Atlantic Oscillation	16	Leaf Area Index	18	Snow melt	32
	Soil moisture (layer 3)	17	Air temperature	15	Evapotranspiration	16	Air temperature	14
	Leaf Area Index	16	Distribution of the rainfall event	15	North Atlantic Oscillation	14	Leaf Area Index	14

In conclusion**,** in the warm season, accumulated antecedent rainfall is an important driver for the four-time scales. Soil moisture is relevant within the two to five days that precede the high flow event. Other drivers such as evapotranspiration and snow melt become relevant between the ten and twenty-days preceding the events.

2. During the cold season

The figure below shows the dominant flood driver in the cold season in the four-time scales.

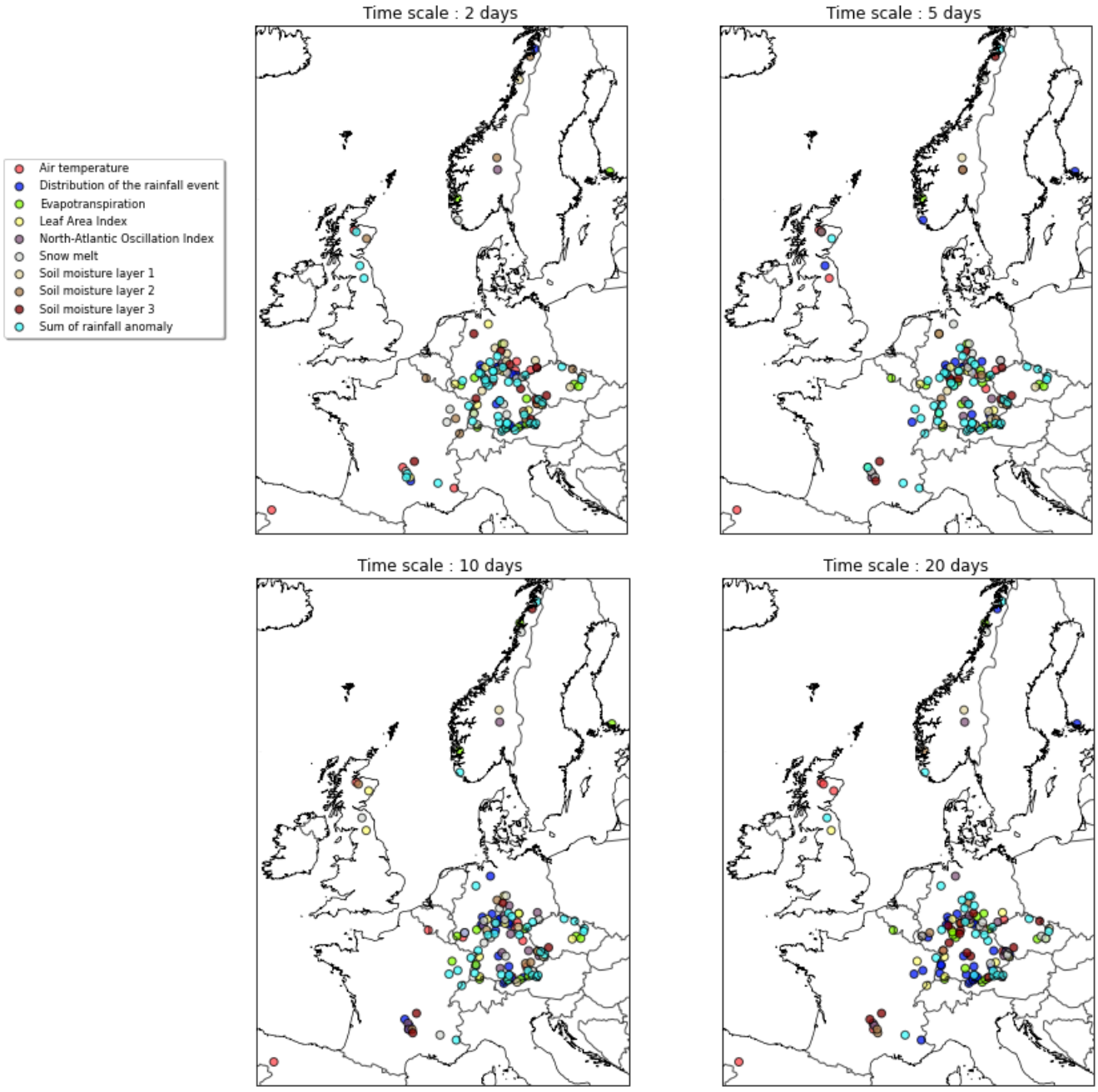

Figure 17 : Dominant flood drivers across different time scales in the cold season

Similarly, to the warm season, accumulated rainfall remains an important driver in all four time-scales as seen in the table below. Compared to the warm season, we notice a higher importance of the distribution of the rainfall event. This means that shorter rainfall events are positively correlated to higher runoff. This importance increases with time in regions like France or Germany.
Snow melt generates floods in shorter time scales (between 2 and 10 days) compared to the warm season. Soil moisture in the first and second layers exerts less of an influence in the cold season compared to the warm season as seen in the table below.

Table 4 : Number of catchments and their associated flood generating mechanism in the cold season

Time scale (days)	2		5		10		20	
Drivers	Accumulated rainfall	39	Accumulated rainfall	41	Accumulated rainfall	31	Distribution of the rainfall event	28
	Distribution of rainfall event	13	Evapotranspiration	18	Distribution of the rainfall event	22	Accumulated rainfall	24
	Evapotranspiration	13	Distribution of the rainfall event	16	Snow melt	16	Evapotranspiration	14
	Snow melt	13	Snow melt	13	Evapotranspiration	15	Soil moisture (layer 3)	13
	Soil moisture (layer 3)	12	North-Atlantic Oscillation Index	11	North Atlantic Oscillation Index	13	North Atlantic Oscillation Index	12

IV. Discussion

Our results demonstrate the role of antecedent rainfall across western Europe in both the warm and cold season and in different time scales that precede a high flow event, in driving streamflow. The analysis found evidence of the role of the upper layers of soil moisture (of depth below 28 cms) between the two and five days that precede a high flow event, in the warm season. This result highlights the role of high soil moisture in the warm season in causing floods despite the high evapotranspiration in this period. It also suggests that floods can possibly be caused by a combined effect of extreme precipitation and low evapotranspiration which translates into high soil moisture. This indicates that floods can be not only be caused by heavy rainfall but are also conditioned by antecedent catchment conditions. This result ties well with previous studies that have identified heavy rainfall with high antecedent soil moisture as the dominant driver of floods in the western parts of Europe (Berghuijs, 2019; Blöschl, 2017; Stein et al, 2019).
It could be argued that precipitation regulates soil moisture, and that floods generated by high soil moisture are inherently conditioned by rainfall. However, other components from the water balance like evapotranspiration also influence water storage (Ghajarnia et al, 2020).
Another finding of the study is the difference in the time scale at which snow melt flood occurs in the warm and cold season. Floods in the warm season in some regions of central Germany are driven by snow melt occurring within the twenty days that precede the flood peak. In the cold season, snow melt occurs on a shorter time scale (between two and five days). This difference could be attributed to catchment properties that can either exacerbate snow melt or not.
Results also show that floods in some catchments located in France and Germany are driven by high evapotranspiration or leaf area index (which is an indicator of interception). Given that precipitation is

partitioned into evapotranspiration, surface runoff or soil storage, it can be hypothesized that in these catchments, soil properties impede water storage due to potential low infiltration capacity. It could also be a spurious correlation due to a low data quality, indicating another flood generating process, for example: air temperature causing both high evapotranspiration and snow melt.

Among the limitations of the study is the fact that the analysis is limited to identifying only one flood generating process per catchment despite the multicausality of floods (see section 3.3 of the Introduction). Moreover, given possible intra-catchment heterogeneity and also differences between various flood events, it can be difficult to attribute one flood process to one catchment.

Using a small sample size to compute correlations and varying station density in different countries can also hinder the interpretability of the results.

In addition, floods can be driven by other mechanisms that have not been selected as drivers in the study. Another aspect is the collinearity or the causal linking between drivers which can distort the correlations computed. As correlations are computed only on a one-to-one basis, this is avoided. However, it is possible that information on a variable is also contained in another variable. One way to assess this would be to compute cross correlations, which can be quite complex with multiple drivers. Use of mixed data sources (modeled and observed) can also lead to possible spurious correlations.

The analysis can be strengthened by using a larger number of catchments to identify more robust spatial patterns in order to counterbalance the issue of statistical significance of the correlations. It is also suggested to dismiss the correlations that do not align with physical processes (i.e., positive correlations between evapotranspiration and runoff, or negative correlations between rainfall and runoff). Given that correlation does not equate causality, a different method to assess flood generating processes like multilinear regression can also be suggested. The method would consist of building multiple models using each driver as a predictor in each model and peak runoff as a target variable. The flood generating mechanism would correspond to the predictor in the best-performing model.

Another limitation of the study is the limited definition of flood. We assumed that peak runoffs correspond to floods without taking into account inundated area. It can be suggested as a follow-up study to use satellite data (NDWI) to validate flood events selected.

V. Summary and conclusion

The study provides a quantitative mapping of the importance of flood drivers in near-natural catchments located in western Europe. A method based on formal attributions in an event-by-event basis of potential flood drivers to runoff anomalies is employed. Relevance of each potential driver is determined using a correlation analysis, over different temporal scales that precede the high flow event.

We highlight the importance of rainfall anomalies in generating floods in this region. In the 172 catchments selected for the study, antecedent rainfall anomalies were the main flood generating process identified in almost 60 catchments in different countries.

This result is particularly important when investigating the possible effects of changes in precipitation in changes of floods. Other factors like soil moisture and snow melt can also generate floods in certain regions, indicating possible combined effects between the identified drivers.

Identifying the relative importance of flood generating mechanisms can reveal regional patterns of causes of floods in Europe and point to processes that require further attention in future studies.

References

ARNELL, N. W, 1994. Variations over time in European hydrological behaviour: a spatial perspective. *FRIEND: Flow Regimes from International Experiment and Network Data*. 1994.

ARNELL, N. W., 2011. Uncertainty in the relationship between climate forcing and hydrological response in UK catchments. *Hydrology and Earth System Sciences*. 15 March 2011. Vol. 15, no. 3, p. 897–912. DOI 10.5194/hess-15-897-2011.

BARREDO, José I., 2007. Major flood disasters in Europe: 1950–2005. *Natural Hazards*. 1 July 2007. Vol. 42, no. 1, p. 125–148. DOI 10.1007/s11069-006-9065-2.

BATES, Paul D., 2004. Remote sensing and flood inundation modelling. *Hydrological Processes*. September 2004. Vol. 18, no. 13, p. 2593–2597. DOI 10.1002/hyp.5649.

BERGHUIJS, Wouter R., HARRIGAN, Shaun, MOLNAR, Peter, SLATER, Louise J. and KIRCHNER, James W., 2019. The Relative Importance of Different Flood-Generating Mechanisms Across Europe. *Water Resources Research*. 2019. Vol. 55, no. 6, p. 4582–4593. DOI 10.1029/2019WR024841.

BEURTON, Susanne and THIEKEN, Annegret H., 2009. Seasonality of floods in Germany. *Hydrological Sciences Journal*. February 2009. Vol. 54, no. 1, p. 62–76. DOI 10.1623/hysj.54.1.62.

BJERKLIE, David M., LAWRENCE DINGMAN, S., VOROSMARTY, Charles J., BOLSTER, Carl H. and CONGALTON, Russell G., 2003. Evaluating the potential for measuring river discharge from space. *Journal of Hydrology*. July 2003. Vol. 278, no. 1–4, p. 17–38. DOI 10.1016/S0022-1694(03)00129-X.

BLÖSCHL, G., NESTER, T., KOMMA, J., PARAJKA, J. and PERDIGÃO, R. a. P., 2013. The June 2013 flood in the Upper Danube Basin, and comparisons with the 2002, 1954 and 1899 floods. *Hydrology and Earth System Sciences*. 20 December 2013. Vol. 17, no. 12, p. 5197–5212. DOI 10.5194/hess-17-5197-2013.

BLÖSCHL, Günter, GAÁL, Ladislav, HALL, Julia, KISS, Andrea, KOMMA, J., NESTER, Thomas, PARAJKA, Juraj, PERDIGAO, Rui, PLAVCOVA, Lenka, ROGGER, Magdalena, SALINAS, José and VIGLIONE, Alberto, 2015. Increasing river floods: Fiction or reality? *Wiley Interdisciplinary Reviews: Water*. 1 March 2015. Vol. 2. DOI 10.1002/wat2.1079.

BLÖSCHL, Günter, HALL, Julia, PARAJKA, Juraj, PERDIGÃO, Rui A. P., MERZ, Bruno, ARHEIMER, Berit, ARONICA, Giuseppe T., BILIBASHI, Ardian, BONACCI, Ognjen, BORGA, Marco, ČANJEVAC, Ivan, CASTELLARIN, Attilio, CHIRICO, Giovanni B., CLAPS, Pierluigi, FIALA, Károly, FROLOVA, Natalia, GORBACHOVA, Liudmyla, GÜL, Ali, HANNAFORD, Jamie, HARRIGAN, Shaun, KIREEVA, Maria, KISS, Andrea, KJELDSEN, Thomas R., KOHNOVÁ, Silvia, KOSKELA, Jarkko J., LEDVINKA, Ondrej, MACDONALD, Neil, MAVROVA-GUIRGUINOVA, Maria, MEDIERO, Luis, MERZ, Ralf, MOLNAR, Peter, MONTANARI, Alberto, MURPHY, Conor, OSUCH, Marzena, OVCHARUK, Valeryia, RADEVSKI, Ivan, ROGGER, Magdalena, SALINAS,

José L., SAUQUET, Eric, ŠRAJ, Mojca, SZOLGAY, Jan, VIGLIONE, Alberto, VOLPI, Elena, WILSON, Donna, ZAIMI, Klodian and ŽIVKOVIĆ, Nenad, 2017. Changing climate shifts timing of European floods. *Science*. 11 August 2017. Vol. 357, no. 6351, p. 588–590. DOI 10.1126/science.aan2506.

BLÖSCHL, Günter, HALL, Julia, VIGLIONE, Alberto, PERDIGÃO, Rui A. P., PARAJKA, Juraj, MERZ, Bruno, LUN, David, ARHEIMER, Berit, ARONICA, Giuseppe T., BILIBASHI, Ardian, BOHÁČ, Miloň, BONACCI, Ognjen, BORGA, Marco, ČANJEVAC, Ivan, CASTELLARIN, Attilio, CHIRICO, Giovanni B., CLAPS, Pierluigi, FROLOVA, Natalia, GANORA, Daniele, GORBACHOVA, Liudmyla, GÜL, Ali, HANNAFORD, Jamie, HARRIGAN, Shaun, KIREEVA, Maria, KISS, Andrea, KJELDSEN, Thomas R., KOHNOVÁ, Silvia, KOSKELA, Jarkko J., LEDVINKA, Ondrej, MACDONALD, Neil, MAVROVA-GUIRGUINOVA, Maria, MEDIERO, Luis, MERZ, Ralf, MOLNAR, Peter, MONTANARI, Alberto, MURPHY, Conor, OSUCH, Marzena, OVCHARUK, Valeryia, RADEVSKI, Ivan, SALINAS, José L., SAUQUET, Eric, ŠRAJ, Mojca, SZOLGAY, Jan, VOLPI, Elena, WILSON, Donna, ZAIMI, Klodian and ŽIVKOVIĆ, Nenad, 2019. Changing climate both increases and decreases European river floods. *Nature*. 5 September 2019. Vol. 573, no. 7772, p. 108–111. DOI 10.1038/s41586-019-1495-6.

BRÁSDIL, R., DOBROVOLNY, P., KAKOS, V., KOTYZA, O., 2006. Historical and recent floods in the Czech Republic: causes, seasonality, trends, impacts. In: Schanze, J., Zeman, E., Marsalek, J. (eds) Flood Risk Management: Hazards, Vulnerability and Mitigation Measures. NATO Science Series, vol 67. Springer, Dordrecht. DOI : 10.1007/978-1-4020-4598-1_20

BUDYKO, M. I and MILLER, David, 1974. *Climate and life*. Online. New York: Academic Press. [Accessed 19 June 2022]. ISBN 978-0-08-095453-0. Available from: https://search.ebscohost.com/login.aspx?direct=true&scope=site&db=nlebk&db=nlabk&AN=297011

CONDON, Laura E., ATCHLEY, Adam L. and MAXWELL, Reed M., 2020. Evapotranspiration depletes groundwater under warming over the contiguous United States. *Nature Communications*. 13 February 2020. Vol. 11, no. 1, p. 873. DOI 10.1038/s41467-020-14688-0.

CORNES, Richard C., VAN DER SCHRIER, Gerard, VAN DEN BESSELAAR, Else J. M. and JONES, Philip D., 2018. An Ensemble Version of the E-OBS Temperature and Precipitation Data Sets. *Journal of Geophysical Research: Atmospheres*. 16 September 2018. Vol. 123, no. 17, p. 9391–9409. DOI 10.1029/2017JD028200.

DETTINGER, Michael and DIAZ, Henry, 2000. Global Characteristics of Stream Flow Seasonality and Variability. *Journal of Hydrometeorology*. 1 August 2000. Vol. 1, p. 289–310. DOI 10.1175/1525-7541(2000)001<0289:GCOSFS>2.0.CO;2.

DI BALDASSARRE, Giuliano, 2012. *Floods in a changing climate. Inundation modelling*. . Cambridge, UK: Cambridge University Press. International hydrology series. ISBN 978-1-107-01875-4.

DÖLL, Petra, 2002. Impact of Climate Change and Variability on Irrigation Requirements: A Global Perspective. *Climatic Change*. August 2002. Vol. 54, no. 3, p. 269–293. DOI 10.1023/A:1016124032231.

DÖLL, Petra, 2009. Vulnerability to the impact of climate change on renewable groundwater resources: a global-scale assessment. *Environmental Research Letters*. July 2009. Vol. 4, no. 3, p. 035006. DOI 10.1088/1748-9326/4/3/035006.

DOOL, H. M. van den, SAHA, S. and JOHANSSON, Å, 2000. Empirical Orthogonal Teleconnections. *Journal of Climate*. 15 April 2000. Vol. 13, no. 8, p. 1421–1435. DOI 10.1175/1520-0442(2000)013<1421:EOT>2.0.CO;2.

DUNNE, Thomas, 1983. Relation of field studies and modeling in the prediction of storm runoff. *Journal of Hydrology*. 1 August 1983. Vol. 65, no. 1, p. 25–48. DOI 10.1016/0022-1694(83)90209-3.

FALLAH, Ali, O, Sungmin and ORTH, Rene, 2020. Climate-dependent propagation of precipitation uncertainty into the water cycle. *Hydrology and Earth System Sciences*. 23 July 2020. Vol. 24, no. 7, p. 3725–3735. DOI 10.5194/hess-24-3725-2020.

FISCHER, Svenja, SCHUMANN, Andreas and BÜHLER, Philipp, 2021. A statistics-based automated flood event separation. *Journal of Hydrology X*. 1 January 2021. Vol. 10, p. 100070. DOI 10.1016/j.hydroa.2020.100070.

GAO, Liping, TAO, Bo, MIAO, Yunxuan, ZHANG, Lihua, SONG, Xia, REN, Wei, HE, Liyuan and XU, Xiaofeng, 2019. A Global Data Set for Economic Losses of Extreme Hydrological Events During 1960-2014. *Water Resources Research*. 2019. Vol. 55, no. 6, p. 5165–5175. DOI 10.1029/2019WR025135.

GHAJARNIA, Navid, KALANTARI, Zahra, ORTH, René and DESTOUNI, Georgia, 2020. Close co-variation between soil moisture and runoff emerging from multi-catchment data across Europe. *Scientific Reports*. 16 March 2020. Vol. 10, no. 1, p. 4817. DOI 10.1038/s41598-020-61621-y.

Global Floods Detection System. Online. [Accessed 31 May 2022]. Available from: https://www.gdacs.org/flooddetection/overview.aspx

GLOBAL RUNOFF DATA CENTRE, 2015. *Twelfth Meeting of the GRDC Steering Committee: 18-19 June 2015, Koblenz, Germany* Online. Bundesanstalt für Gewässerkunde, Koblenz. [Accessed 29 May 2022].

GUDMUNDSSON, Lukas, DO, Hong Xuan, LEONARD, Michael and WESTRA, Seth, 2018. The Global Streamflow Indices and Metadata Archive (GSIM) – Part 2: Quality control, time-series indices and homogeneity assessment. *Earth System Science Data*. 17 April 2018. Vol. 10, no. 2, p. 787–804. DOI 10.5194/essd-10-787-2018.

GUPTA, H. V., PERRIN, C., BLÖSCHL, G., MONTANARI, A., KUMAR, R., CLARK, M. and ANDRÉASSIAN, V., 2014. Large-sample hydrology: a need to balance depth with breadth. *Hydrology and Earth System Sciences*. 6 February 2014. Vol. 18, no. 2, p. 463–477. DOI 10.5194/hess-18-463-2014.

HALL, J., ARHEIMER, B., ARONICA, G. T., BILIBASHI, A., BOHÁČ, M., BONACCI, O., BORGA, M., BURLANDO, P., CASTELLARIN, A., CHIRICO, G. B., CLAPS, P., FIALA, K., GAÁL, L., GORBACHOVA, L., GÜL, A., HANNAFORD, J., KISS, A., KJELDSEN, T., KOHNOVÁ,

S., KOSKELA, J. J., MACDONALD, N., MAVROVA-GUIRGUINOVA, M., LEDVINKA, O., MEDIERO, L., MERZ, B., MERZ, R., MOLNAR, P., MONTANARI, A., OSUCH, M., PARAJKA, J., PERDIGÃO, R. a. P., RADEVSKI, I., RENARD, B., ROGGER, M., SALINAS, J. L., SAUQUET, E., ŠRAJ, M., SZOLGAY, J., VIGLIONE, A., VOLPI, E., WILSON, D., ZAIMI, K. and BLÖSCHL, G., 2015. A European Flood Database: facilitating comprehensive flood research beyond administrative boundaries. In: *Proceedings of IAHS*. Online. Copernicus GmbH. 11 June 2015. p. 89–95. [Accessed 20 June 2022]. DOI 10.5194/piahs-370-89-2015.

HALL, Julia and BLÖSCHL, Günter, 2018. Spatial patterns and characteristics of flood seasonality in Europe. *Hydrology and Earth System Sciences*. 19 July 2018. Vol. 22, no. 7, p. 3883–3901. DOI 10.5194/hess-22-3883-2018.

HANNAFORD, Jamie and HALL, Jim W., 2012. Flood Risk in the UK: Evidence of Change and Management Responses. In: *Changes in Flood Risk in Europe*. CRC Press. ISBN 978-0-203-09809-7.

HANNAH, David M, FLEIG, Anne K, KINGSTON, Daniel G, STAGGE, James H and WILSON, Donna, 2014. Connecting streamflow and atmospheric conditions in Europe: state-of-the-art review and future directions. . 2014. P. 6.

HIRSCHBOECK, K. K., 1988. Flood hydroclimatology. *Nuclear Physics A*. 1988. P. 27–49.

HIRSCHBOECK, K. K., 1991. Climate and floods. . 1991. Vol. 2375, p. 67–88.

HORTON, 1931. The field, scope, and status of the science of hydrology. *Eos, Transactions American Geophysical Union*. 1931. Vol. 12, no. 1, p. 189–202. DOI 10.1029/TR012i001p00189-2.

IVANCIC, Timothy J. and SHAW, Stephen B., 2015. Examining why trends in very heavy precipitation should not be mistaken for trends in very high river discharge. *Climatic Change*. December 2015. Vol. 133, no. 4, p. 681–693. DOI 10.1007/s10584-015-1476-1.

JARRAUD, M and BOKOVA, I, International Glossary of Hydrology. . P. 471.

KINGSTON, Daniel, MASSEI, Nicolas, DIEPPOIS, Bastien, HANNAH, David, HARTMANN, Andreas, LAVERS, David and VIDAL, Jean-Philippe, 2020. Moving beyond the catchment scale: Value and opportunities in large-scale hydrology to understand our changing world. *Hydrological Processes*. May 2020. Vol. 34, no. 10, p. 2292–2298. DOI 10.1002/hyp.13729.

KRASOVSKAIA, I., ARNELL, N. W. & GOTTSCHALK, L, Krasovskaia, 1994. Flow regimes in northern and western Europe: development and application of procedures for classifying flow regimes. *IAHS*. Vol. FRIEND: Flow Regimes from International Experimental and Network Data, no. 221, p. 185–223.

KUNDZEWICZ, Zbigniew W, 2007. Freshwater Resources and Their Management. In: Parry, M.L., Canziani, O.F., Palutikof, J.P., van der Linden, P.J. and Hanson, C.E., Eds., Climate Change 2007: Working Group II: Impacts, Adaptation and Vulnerability, Cambridge University Press, Cambridge, 173-210.

KUNDZEWICZ, Zbigniew W. and KACZMAREK, Zdzislaw, 2000. Coping with Hydrological Extremes. *Water International*. March 2000. Vol. 25, no. 1, p. 66–75. DOI 10.1080/02508060008686798.

LAIZÉ, Cédric L. R. and HANNAH, David M., 2010. Modification of climate–river flow associations by basin properties. *Journal of Hydrology*. 28 July 2010. Vol. 389, no. 1, p. 186–204. DOI 10.1016/j.jhydrol.2010.05.048.

LINS, Harry F, 2006. Observed Trends in Hydrologic Cycle Components. In: *Encyclopedia of Hydrological Sciences*. Online. John Wiley & Sons, Ltd. [Accessed 5 June 2022]. ISBN 978-0-470-84894-4.

MANFREDA, Salvatore, IACOBELLIS, Vito, GIOIA, Andrea, FIORENTINO, Mauro and KOCHANEK, Krzysztof, 2018. The Impact of Climate on Hydrological Extremes. *Water*. June 2018. Vol. 10, no. 6, p. 802. DOI 10.3390/w10060802.

MARSH, Terry, 2008. A hydrological overview of the summer 2007 floods in England and Wales. *Weather*. 2008. Vol. 63, no. 9, p. 274–279. DOI 10.1002/wea.305.

MARTENS, Brecht, MIRALLES, Diego G., LIEVENS, Hans, VAN DER SCHALIE, Robin, DE JEU, Richard A. M., FERNÁNDEZ-PRIETO, Diego, BECK, Hylke E., DORIGO, Wouter A. and VERHOEST, Niko E. C., 2017. GLEAM v3: satellite-based land evaporation and root-zone soil moisture. *Geoscientific Model Development*. 17 May 2017. Vol. 10, no. 5, p. 1903–1925. DOI 10.5194/gmd-10-1903-2017.

MASSON-DELMOTTE, V., P. ZHAI, A. PIRANI, S.L., CONNORS, C. PÉAN, S. BERGER, N. CAUD, Y. CHEN, L. GOLDFARB, M.I. GOMIS, M. HUANG, K. LEITZELL, E. LONNOY, J.B.R., and MATTHEWS, T.K. MAYCOCK, T. WATERFIELD, O. YELEKÇI, R. YU, AND B. ZHOU (EDS.), 2021. *IPCC, 2021 : Climate Change 2021: The Physical Science Basis. Contribution of Working Group I to the Sixth Assessment Report of the Intergovernmental Panel on Climate Change*. Online. Cambridge University Press. Available from: doi:10.1017/9781009157896.001.

MERZ, B., THIEKEN, A.H. and GOCHT, M., 2007. Flood Risk Mapping At The Local Scale: Concepts and Challenges. In: BEGUM, Selina, STIVE, Marcel J. F. and HALL, Jim W. (eds.), *Flood Risk Management in Europe: Innovation in Policy and Practice*. Online. Dordrecht: Springer Netherlands. p. 231–251. Advances in Natural and Technological Hazards Research. [Accessed 19 June 2022]. ISBN 978-1-4020-4200-3.

MERZ, Bruno, BLÖSCHL, Günter, VOROGUSHYN, Sergiy, DOTTORI, Francesco, AERTS, Jeroen C. J. H., BATES, Paul, BERTOLA, Miriam, KEMTER, Matthias, KREIBICH, Heidi, LALL, Upmanu and MACDONALD, Elena, 2021. Causes, impacts and patterns of disastrous river floods. *Nature Reviews Earth & Environment*. September 2021. Vol. 2, no. 9, p. 592–609. DOI 10.1038/s43017-021-00195-3.

MERZ, R. and BLÖSCHL, G., 2003. A process typology of regional floods. *Water Resources Research*. Online. 2003. Vol. 39, no. 12. [Accessed 16 June 2022]. DOI 10.1029/2002WR001952.

NAUMANN, Gustavo, SPINONI, Jonathan, VOGT, Jürgen V. and BARBOSA, Paulo, 2015. Assessment of drought damages and their uncertainties in Europe. *Environmental Research Letters*. December 2015. Vol. 10, no. 12, p. 124013. DOI 10.1088/1748-9326/10/12/124013.

NEWMAN, A. J., CLARK, M. P., SAMPSON, K., WOOD, A., HAY, L. E., BOCK, A., VIGER, R. J., BLODGETT, D., BREKKE, L., ARNOLD, J. R., HOPSON, T. and DUAN, Q., 2015. Development of a large-sample watershed-scale hydrometeorological data set for the contiguous USA: data set characteristics and assessment of regional variability in hydrologic model performance. *Hydrology and Earth System Sciences*. 14 January 2015. Vol. 19, no. 1, p. 209–223. DOI 10.5194/hess-19-209-2015.

O, Sungmin, DUTRA, Emanuel and ORTH, Rene, 2020. Robustness of Process-Based versus Data-Driven Modeling in Changing Climatic Conditions. *Journal of Hydrometeorology*. 1 September 2020. Vol. 21, no. 9, p. 1929–1944. DOI 10.1175/JHM-D-20-0072.1.

ORTH, Rene, O, Sungmin, ZSCHEISCHLER, Jakob, MAHECHA, Miguel D. and REICHSTEIN, Markus, 2022. Contrasting biophysical and societal impacts of hydro-meteorological extremes. *Environmental Research Letters*. January 2022. Vol. 17, no. 1, p. 014044. DOI 10.1088/1748-9326/ac4139.

ORTH, Rene and SENEVIRATNE, Sonia I., 2015. Introduction of a simple-model-based land surface dataset for Europe. *Environmental Research Letters*. April 2015. Vol. 10, no. 4, p. 044012. DOI 10.1088/1748-9326/10/4/044012.

POTTER, N. J., ZHANG, L., MILLY, P. C. D., MCMAHON, T. A. and JAKEMAN, A. J., 2005. Effects of rainfall seasonality and soil moisture capacity on mean annual water balance for Australian catchments. *Water Resources Research*. Online. 2005. Vol. 41, no. 6. [Accessed 29 May 2022]. DOI 10.1029/2004WR003697.

PRUDHOMME, Christel and GENEVIER, Marie, 2011. Can atmospheric circulation be linked to flooding in Europe? *Hydrological Processes*. 2011. Vol. 25, no. 7, p. 1180–1190. DOI 10.1002/hyp.7879.

SCHAAKE ET AL, 2001. Toward improvement parameter-estimation of land surface hydrology models through the Model Parameter Estimation Experiment (MOPEX). *IAHS-AISH Publ.* 2001. Vol. 270, p. 91–98.

SCHRÖTER, K., KUNZ, M., ELMER, F., MÜHR, B. and MERZ, B., 2015. What made the June 2013 flood in Germany an exceptional event? A hydro-meteorological evaluation. *Hydrology and Earth System Sciences*. 16 January 2015. Vol. 19, no. 1, p. 309–327. DOI 10.5194/hess-19-309-2015.

Série de variables végétales (GEOV2-AVHRR) – Theia, [no date]. Online. [Accessed 10 June 2022]. Available from: https://www.theia-land.fr/product/serie-de-variables-vegetales-avhrr-fr/

SHARMA, Ashish, WASKO, Conrad and LETTENMAIER, Dennis P., 2018. If Precipitation Extremes Are Increasing, Why Aren't Floods? *Water Resources Research*. November 2018. Vol. 54, no. 11, p. 8545–8551. DOI 10.1029/2018WR023749.

SHORTHOUSE, C. and ARNELL, N., 1999. The effects of climatic variability on spatial characteristics of European river flows. *Physics and Chemistry of the Earth, Part B: Hydrology, Oceans and Atmosphere*. 1 January 1999. Vol. 24, no. 1, p. 7–13. DOI 10.1016/S1464-1909(98)00003-3.

SHORTHOUSE, CORDELIA & ARNELL, NIGEL., Shorthouse, 1997. Spatial and temporal variability in European river flows and the North Atlantic Oscillation. *IAHS-AISH Publication*. 1997. No. 246.

STAHL K, HISDAL H (ed.), 2004. *Hydroclimatology*. . 1. ed., Reprint. Amsterdam Heidelberg: Elsevier. Developments in water science, 48. ISBN 978-0-444-51767-8.

STAHL, K., HISDAL, H., HANNAFORD, J., TALLAKSEN, L. M., VAN LANEN, H. a. J., SAUQUET, E., DEMUTH, S., FENDEKOVA, M. and JÓDAR, J., 2010. Streamflow trends in Europe: evidence from a dataset of near-natural catchments. *Hydrology and Earth System Sciences*. 1 December 2010. Vol. 14, no. 12, p. 2367–2382. DOI 10.5194/hess-14-2367-2010.

STEIN, L., CLARK, M. P., KNOBEN, W. J. M., PIANOSI, F. and WOODS, R. A., 2021. How Do Climate and Catchment Attributes Influence Flood Generating Processes? A Large-Sample Study for 671 Catchments Across the Contiguous USA. *Water Resources Research*. 2021. Vol. 57, no. 4, p. e2020WR028300. DOI 10.1029/2020WR028300.

TARASOVA, Larisa, MERZ, Ralf, KISS, Andrea, BASSO, Stefano, BLÖSCHL, Günter, MERZ, Bruno, VIGLIONE, Alberto, PLÖTNER, Stefan, GUSE, Björn, SCHUMANN, Andreas, FISCHER, Svenja, AHRENS, Bodo, ANWAR, Faizan, BÁRDOSSY, András, BÜHLER, Philipp, HABERLANDT, Uwe, KREIBICH, Heidi, KRUG, Amelie, LUN, David, MÜLLER-THOMY, Hannes, PIDOTO, Ross, PRIMO, Cristina, SEIDEL, Jochen, VOROGUSHYN, Sergiy and WIETZKE, Luzie, 2019. Causative classification of river flood events. *WIREs Water*. 2019. Vol. 6, no. 4, p. e1353. DOI 10.1002/wat2.1353.

TIM DAVIE, 2019. *Fundamentals of Hydrology*. Online. [Accessed 31 May 2022]. ISBN 978-0-415-85870-0. Available from: https://www.routledge.com/Fundamentals-of-Hydrology/Davie/p/book/9780415858700

VEN TE CHOW, Ven Te Chow, 1956. *Hydrologic Studies of Floods in the United States*. . Association Internationale d'Hydrologie.

WARD R. C., 1978. *Floods—A geographical perspective*. Online. London: The Macmillan Press. [Accessed 19 June 2022]. Available from: https://onlinelibrary.wiley.com/doi/10.1002/esp.3290040320

WOHL, Ellen E. (ed.), 2000. *Inland flood hazards: human, riparian, and aquatic communities*. . Cambridge ; New York, NY: Cambridge University Press. ISBN 978-0-521-62419-0.

WOLOCK, David M. and MCCABE, Gregory J., 1999. Explaining spatial variability in mean annual runoff in the conterminous United States. *Climate Research*. 22 March 1999. Vol. 11, no. 2, p. 149–159. DOI 10.3354/cr011149.

Appendix

A.1. Catchment information

EWA_ID	Country	Basin area (km^2)	Latitude	Longitude	Site	River
CZ_1430	CZ	383.4	49.2	13.89	Nemetice	Volynka
CZ_1550	CZ	131.9	49.555	15.849	Sázava	Sázava
CZ_180	CZ	248.07	50.48	16.18	Hronov	Metuji
CZ_3450	CZ	349.8	50.04	16.91	Raskov	Morava
CZ_3540	CZ	444.54	49.89	16.84	Lupene	Moravska Sazava
CZ_4410	CZ	128.1	49.68	16.19	Borovnice	Svratka
CZ_4540	CZ	419.31	49.54	16.54	Letovice	Svitava
CZ_900	CZ	179.76	50.66	15.33	Bohunovsko-Jesenny	Kamenice
ES_1734	ES	558	42.413	-6.816	Puente De Domingo Florez	Cabrera
ES_2089	ES	280	42.224	-6.251	Morla	Eria
ES_9063	ES	506	42.632	-1.012	Sigües	Esca
ES_9079	ES	180	42.773	-1.434	Urroz	Erro
FI_2228002	FI	730	60.464	22.309	Halinen	Aurajoki
FR_A3472010	FR	688	48.75	7.634	Waltenheim-Sur-Zorn	La Zorn
FR_A4200630	FR	621	48.066	6.611	St-Nabord (Noir Gueux)	La Moselle
FR_A5431010	FR	940	48.545	6.133	Pulligny	Le Madon
FR_D0156510	FR	198	50.118	4.079	Liessies	L' Helpe Majeure
FR_E3511220	FR	158	50.618	2.216	Delettes	La Lys
FR_E4035710	FR	392	50.708	2.245	Wizernes	L' Aa
FR_H0400010	FR	2340	48.117	4.378	Bar-Sur-Seine	La Seine
FR_K1503010	FR	135	46.127	3.682	Chatel-Montagne	La Besbre
FR_K2523010	FR	310	45.138	3.004	Neussargues-Moissac (Joursac-Le-Vialard)	L' Alagnon
FR_K2871910	FR	800	45.694	3.595	Tours-Sur-Meymont (Giroux)	La Dore
FR_K5183010	FR	854	46.185	2.434	Evaux-Les-Bains	La Tardes
FR_L0140610	FR	1156	45.884	1.4	St-Priest-Taurion	La Vienne
FR_L0231510	FR	388	45.994	1.844	Pontarion	Le Taurion
FR_L4010710	FR	165	45.881	2.171	Felletin	La Creuse
FR_L4033010	FR	186	45.92	2.23	Moutier-Rozeille (Auloussou)	La Rozeille
FR_L4220710	FR	1235	46.377	1.677	Fresselines	La Grande Creuse
FR_L4411710	FR	850	46.384	1.685	Fresselines (Puy Rageaud)	La Petite Creuse
FR_O5292510	FR	1540	44.153	1.972	Laguepie (1)	L' Aveyron
FR_O5572910	FR	1530	44.143	1.969	Laguepie	Le Viaur
FR_O7054010	FR	89	44.652	3.414	St-Amans (Ganivet)	La Colagne
FR_O7101510	FR	1160	44.439	3.194	Banassac (La Mothe)	Le Lot
FR_O7272510	FR	542	44.835	3.348	Malzieu-Ville (Le Soulier)	La Truyere

FR_O7354010	FR	310	45.012	3.13	St-Georges	La Lander
FR_O7444010	FR	283	44.826	3.087	St-Juery	Le Bes
FR_P0364010	FR	172	45.333	2.753	Condat (Roche-Pointue)	La Santoire
FR_P0894010	FR	401	45.3	2.386	Bassignac (Pont De Vendes)	La Sumene
FR_P1502510	FR	513	45.083	2.195	Pleaux (Enchanet)	La Maronne
FR_P3021010	FR	143	45.604	1.925	Bugeat	La Vezere
FR_U0230010	FR	1130	47.858	5.932	Cendrecourt	La Saone
FR_U2122010	FR	1060	47.272	6.951	Goumois	Le Doubs
FR_V4214010	FR	194	44.619	5.445	Luc-En-Diois	La Drome
FR_X0434010	FR	549	44.385	6.653	Barcelonnette (Abattoir)	L' Ubaye
FR_Y2015010	FR	159	44	3.659	Vigan (La Terrisse)	L' Arre
FR_Y5615020	FR	140	43.721	6.979	Gourdon (Loup-Amont)	Le Loup
DE_120001440	DE	308.1	47.87	10.04	Lauben	Aitrach
DE_120001470	DE	126	48.84	10.41	Trochtelfingen	Eger
DE_120001920	DE	81	48.2	9.96	Tuttlingen	Elta
DE_120002110	DE	282.8	49.55	8.68	Archshofen	Tauber
DE_120003570	DE	617	47.63	8.33	Oberlauchringen	Wutach
DE_120003640	DE	49.3	47.75	8.35	Illmuehle	Steina
DE_120003750	DE	26	48.34	8.05	Wehr-Hasel	Hasel
DE_120003860	DE	39.8	47.94	7.95	Oberried-Ibrech	Brugga
DE_120003900	DE	957	48.39	8.03	Schwaibach	Kinzig
DE_120004730	DE	245.7	49.02	10.12	Abtsgmuend	Lein
DE_120013010	DE	468.8	48.82	8.3	Rotenfels	Murg
DE_120014390	DE	137.6	48.85	9.84	Geislingen - Fils	Fils
DE_11418001	DE	117	47.41	10.23	Breitachklamm	Breitach
DE_11942009	DE	133	48.29	10.65	Fischach	Schmutter
DE_12183005	DE	110	47.58	10.56	Pfronten Ried	Vils
DE_12186003	DE	22.3	47.56	10.52	Fallmuehle	Steinacher Ache
DE_12326000	DE	25	47.65	10.83	Trauchgau	Trauchgauer Ach
DE_12335001	DE	32.2	47.73	10.89	Engen	Illach
DE_12405005	DE	450	47.83	10.65	Biessenhofen	Wertach
DE_12445000	DE	95.4	47.83	10.66	Hoermannshofen	Geltnach
DE_14601004	DE	98.9	49.63	11.83	Gressenwoehr	Vils
DE_15214003	DE	177	49.03	13.23	Zwiesel	Grosser Regen
DE_15218004	DE	109	49.04	13	Teisnach	Teisnach
DE_15243001	DE	276	49.09	12.27	Furth Im Wald	Chamb
DE_15993001	DE	36.3	48.8	13.09	Deggendorf	Kollbach
DE_16000708	DE	400	47.45	11.27	Mittenwald Karwendel	Isar
DE_16312008	DE	7.6	47.59	11.54	Sylvenstein	Schronbach
DE_16825002	DE	141.8	48.42	11.98	Appolding	Strogen

DE_17215007	DE	318	48.47	12.39	Vilsbiburg	Grosse Vils
DE_17345002	DE	212	48.73	13.44	Hoerrmannsberg	Gaissa
DE_17404000	DE	363	48.94	13.41	Schrottenbaummuehle	Ilz
DE_17425000	DE	113	48.83	13.36	Eberhardsreuth	Mitternacher Oh
DE_17466007	DE	60.6	48.85	13.54	Unterkashof	Reschwasser
DE_17468002	DE	120	49.01	13.24	Roehrnbach	Osterbach
DE_18196000	DE	30.1	47.75	12.18	Nussdorf	Steinbach
DE_18216005	DE	31.3	47.69	11.78	Rottach	Rottach
DE_18346000	DE	244	48.03	12.15	Anger	Attel
DE_18381500	DE	59.5	48.25	12.04	Weg	Isen
DE_18454003	DE	944	47.78	12.48	Staudach	Tiroler Achen
DE_18483500	DE	378	47.99	12.55	Stein Bei Altenmarkt	Traun
DE_18642003	DE	940	47.69	12.82	Unterjettenberg Rech	Saalach
DE_18646809	DE	49.9	47.77	12.92	Piding	Stoisser Ache
DE_24118500	DE	65	50.18	11.53	Oberhammer	Untere Steinach
DE_24123000	DE	333	49.95	11.57	Bayreuth	Roter Main
DE_24140509	DE	56.1	50.36	11.51	Streitmuehle Bei Due	Rodach
DE_24186000	DE	383	50.01	10.85	Leucherhof	Baunach
DE_24482003	DE	457	50.2	9.62	Mittelsinn	Sinn
DE_24522006	DE	220	50.03	9.54	Partenstein	Lohr
DE_24752006	DE	142	49.83	9.22	Rueck	Elsava
DE_56122008	DE	84	50.25	12.02	Rehau	Schwesnitz
DE_24762653	DE	461	49.97	8.99	Harreshausen	Gersprenz
DE_24784259	DE	921	50.13	8.95	Hanau	Kinzig
DE_24861407	DE	392.6	50.23	8.88	Windecken	Nidder
DE_25810558	DE	304.2	50.91	8.53	Biedenkopf	Lahn
DE_25822808	DE	916.3	50.8	8.94	Hainmuehle	Ohm
DE_25831059	DE	81.2	50.72	8.65	Etzelmuehle	Salzboede
DE_25832357	DE	23.5	50.46	8.6	Oberkleen	Cleebach
DE_25850257	DE	98.6	50.5	8.43	Bonbaden	Solmsbach
DE_25880305	DE	143.7	50.24	8.06	Michelbach	Aar
DE_41450056	DE	182	50.66	10.01	Guenthers	Ulster
DE_42350057	DE	561	50.6	9.64	Kaemmerzell	Fulda
DE_42810204	DE	489.7	50.59	9.59	Auhammer	Eder
DE_42882806	DE	986.1	51.07	9.33	Uttershausen	Schwalm
DE_3637101	DE	958	52.56	7.95	Bersenbruck	Hase
DE_4823104	DE	363	52.03	10.55	Schladen	Oker
DE_4882168	DE	129	51.65	10.26	Hattorf	Sieber
DE_4884110	DE	149	51.81	9.77	Oldendorf	Iilme
DE_4886122	DE	212	52.02	10.37	Hohenrode	Innerste
DE_4945108	DE	908	53.08	9.21	Hellwege Schl. V	Wumme
DE_23750306	DE	101	49.14	8.2	Herxheim	Klinbach
DE_26280854	DE	266	49.88	6.46	Alsdorf-Oberecken	Nims
DE_26760306	DE	170	49.83	6.94	Papiermuhle	Dhron
DE_26840507	DE	176	50.07	7.08	Peltzerhaus	Uessbach

DE_563790	DE	362	50.59	12.71	Aue1	Schwarzwasser
DE_567320	DE	286	51.08	13.15	Niederstriegis1	Striegis
DE_568140	DE	385	50.7	13.24	Pockau1	Floeha
DE_576400	DE	171	50.33	12.26	Adorf	Weisse Elster
DE_252460	DE	42.1	50.405	11.206	Hüttengrund	Engnitz
DE_420020	DE	1170	50.575	10.417	Meiningen	Werra
DE_421620	DE	114	50.509	10.746	Schleusingen	Nahe
DE_422000	DE	321	50.608	10.678	Ellingshausen	Hasel
DE_425120	DE	29.8	50.787	10.41	Trusetal	Truse
DE_426000	DE	214	50.824	10.082	Dorndorf 2	Felda
DE_427010	DE	399	50.808	9.978	Unterbreizbach	Ulster
DE_429010	DE	305.2	50.976	10.345	Eisenach-Petersberg	Hörsel
DE_447000	DE	275	51.38	9.972	Arenshausen	Leine
DE_572010	DE	362.3	50.603	11.446	Kaulsdorf-Eichicht	Loquitz
DE_572920	DE	894.3	51.073	11.581	Niedertrebra	Ilm
DE_573010	DE	716.1	51.108	10.713	Nägelstedt	Unstrut
DE_574210	DE	842.8	50.926	10.989	Erfurt-Möbisburg	Gera
DE_575500	DE	303.6	51.508	10.785	Nordhausen	Zorge
NL_1000	NL	351.1	52.05	6.45	Ammeloe	Berkel
NO_1702008	NO	465	61.852	10.222	Atnasjø	Glomma
NO_1702033	NO	866	61.216	10.271	Aulestad	Jøra
NO_1727004	NO	185	58.534	6.15	Helleland	Ogna
NO_1741001	NO	129	59.683	6.011	Stordalsvatn	Etneelv
NO_1852001	NO	520	65.905	13.308	Fustvatn	Fusta
NO_1857002	NO	16.1	66.393	13.181	Vassvatn	Kjerringå
NO_1862001	NO	144	67.084	14.983	Skarsvatn	Lakselv
NO_1866001	NO	230.3	67.451	15.761	Lakshola	Lakså
UK_12001	UK	1370	57.05	-2.602	Woodend	Dee
UK_18001	UK	161	56.225	-3.949	Kinbuck	Allan Water
UK_21006	UK	1500	55.592	-2.797	Boleside	Tweed
UK_23004	UK	751.1	54.977	-2.225	Haydon Bridge	South Tyne
UK_24004	UK	74.9	54.685	-1.817	Bedburn	Bedburn Beck
UK_25006	UK	86.1	54.505	-1.947	Rutherford Bridge	Greta
UK_28008	UK	399	52.95	-1.83	Rocester Weir	Dove
UK_32003	UK	74.3	52.408	-0.555	Old Mill Bridge	Harpers Brook
UK_33012	UK	137.5	52.254	-0.308	Meagre Farm	Kym
UK_33019	UK	316	52.412	0.765	Melford Bridge	Thet
UK_39020	UK	106.7	51.754	-1.823	Bibury	Coln
UK_39054	UK	31.8	51.144	-0.199	Gatwick Airport	Mole
UK_42003	UK	98.9	50.815	-1.549	Brockenhurst	Lymington
UK_50002	UK	663	50.946	-4.135	Torrington	Torridge
UK_53006	UK	148.9	51.49	-2.52	Frenchay	Frome(Bristol)
UK_54008	UK	1134.4	52.314	-2.591	Tenbury	Teme
UK_55026	UK	174	52.297	-3.502	Ddol Farm	Wye
UK_57004	UK	106	51.651	-3.331	Abercynon	Cynon

UK_60002	UK	297.9	51.88	-4.17	Felin Mynachdy	Cothi
UK_68005	UK	207	52.984	-2.517	Audlem	Weaver
UK_7001	UK	415.6	57.379	-3.953	Shenachie	Findhorn
UK_71001	UK	1145	53.777	-2.627	Samlesbury	Ribble
UK_78004	UK	76.1	55.167	-3.449	Redhall	Kinnel Water
UK_79002	UK	799	55.148	-3.69	Friars Carse	Nith
UK_8009	UK	272.2	57.302	-3.698	Balnaan Bridge	Dulnain

A.2. Nash-Sutcliffe Efficiency from the Simple Water Balance Model

Catchment ID	NSE
CZ_1430	0.459
CZ_1550	0.421
CZ_180	0.507
CZ_3450	0.396
CZ_3540	0.589
CZ_4410	0.578
CZ_4540	0.361
CZ_900	0.377
ES_1734	0.656
ES_2089	0.430
ES_9063	0.388
ES_9079	0.477
FI_2228002	0.396
FR_A3472010	0.509
FR_A4200630	0.642
FR_A5431010	0.534
FR_D0156510	0.593
FR_E3511220	0.599
FR_E4035710	0.467
FR_H0400010	0.655
FR_K1503010	0.407
FR_K2523010	0.405
FR_K2871910	0.492
FR_K5183010	0.541
FR_L0140610	0.611
FR_L0231510	0.617
FR_L4010710	0.542
FR_L4033010	0.629
FR_L4220710	0.712
FR_L4411710	0.566
FR_O5292510	0.482
FR_O5572910	0.495

FR_O7054010	0.582
FR_O7101510	0.390
FR_O7272510	0.511
FR_O7354010	0.383
FR_O7444010	0.381
FR_P0364010	0.485
FR_P0894010	0.487
FR_P1502510	0.639
FR_P3021010	0.594
FR_U0230010	0.537
FR_U2122010	0.677
FR_V4214010	0.483
FR_X0434010	0.369
FR_Y2015010	0.486
FR_Y5615020	0.393
DE_120001440	0.527
DE_120001470	0.595
DE_120001920	0.421
DE_120002110	0.364
DE_120003570	0.599
DE_120003640	0.571
DE_120003750	0.430
DE_120003860	0.634
DE_120003900	0.653
DE_120004730	0.760
DE_120013010	0.532
DE_120014390	0.529
DE_11418001	0.418
DE_11942009	0.385
DE_12183005	0.471
DE_12186003	0.472
DE_12326000	0.371
DE_12335001	0.360
DE_12405005	0.633
DE_12445000	0.508
DE_14601004	0.509
DE_15214003	0.464
DE_15218004	0.476
DE_15243001	0.410
DE_15993001	0.569
DE_16000708	0.552
DE_16312008	0.405
DE_16825002	0.415
DE_17215007	0.463
DE_17345002	0.625

DE_17404000	0.396
DE_17425000	0.466
DE_17466007	0.508
DE_17468002	0.453
DE_18196000	0.402
DE_18216005	0.525
DE_18346000	0.443
DE_18381500	0.384
DE_18454003	0.472
DE_18483500	0.465
DE_18642003	0.471
DE_18646809	0.544
DE_24118500	0.712
DE_24123000	0.447
DE_24140509	0.759
DE_24186000	0.634
DE_24482003	0.752
DE_24522006	0.771
DE_24752006	0.651
DE_56122008	0.653
DE_24762653	0.467
DE_24784259	0.564
DE_24861407	0.586
DE_25810558	0.713
DE_25822808	0.467
DE_25831059	0.651
DE_25832357	0.495
DE_25850257	0.488
DE_25880305	0.548
DE_41450056	0.607
DE_42350057	0.702
DE_42810204	0.484
DE_42882806	0.647
DE_3637101	0.387
DE_4823104	0.559
DE_4882168	0.529
DE_4884110	0.696
DE_4886122	0.635
DE_4945108	0.510
DE_23750306	0.361
DE_26280854	0.634
DE_26760306	0.701
DE_26840507	0.660
DE_563790	0.492
DE_567320	0.688

DE_568140	0.520
DE_576400	0.673
DE_252460	0.609
DE_420020	0.645
DE_421620	0.713
DE_422000	0.672
DE_425120	0.527
DE_426000	0.695
DE_427010	0.636
DE_429010	0.593
DE_447000	0.707
DE_572010	0.644
DE_572920	0.555
DE_573010	0.511
DE_574210	0.655
DE_575500	0.554
NL_1000	0.400
NO_1702008	0.664
NO_1702033	0.383
NO_1727004	0.629
NO_1741001	0.686
NO_1852001	0.600
NO_1857002	0.518
NO_1862001	0.406
NO_1866001	0.464
UK_12001	0.411
UK_18001	0.588
UK_21006	0.727
UK_23004	0.531
UK_24004	0.554
UK_25005	0.435
UK_25006	0.554
UK_28008	0.613
UK_32003	0.434
UK_33012	0.394
UK_33019	0.476
UK_39020	0.619
UK_39054	0.628
UK_42003	0.622
UK_50002	0.685
UK_53006	0.467
UK_54008	0.577
UK_55026	0.636
UK_57004	0.501
UK_60002	0.545

UK_68005	0.411
UK_7001	0.421
UK_71001	0.668
UK_78004	0.708
UK_79002	0.723
UK_8009	0.439
UK_81002	0.447

A.3. Correlations of important flood drivers in the time scale of two days in the warm season

EWA_ID	Drivers	Spearman's rho	River
CZ_1430	Soil moisture layer 1	0.600	Volynka
CZ_1550	Soil moisture layer 2	0.673	Sázava
CZ_180	Sum of rainfall anomaly	0.709	Metuji
CZ_3450	Soil moisture layer 2	0.733	Morava
CZ_3540	Sum of rainfall anomaly	0.758	Moravska Sazava
CZ_4410	Sum of rainfall anomaly	0.648	Svratka
CZ_4410	Leaf Area Index	0.648	Svitava
CZ_4540	Soil moisture layer 1	0.576	Kamenice
CZ_900	Soil moisture layer 1	0.782	Cabrera
ES_1734	Soil moisture layer 2	0.612	Eria
ES_2089	Soil moisture layer 2	0.794	Esca
ES_9063	Sum of rainfall anomaly	0.503	Erro
ES_9079	Soil moisture layer 2	0.588	Aurajoki
FI_2228002	Sum of rainfall anomaly	0.321	La Zorn
FR_A3472010	Sum of rainfall anomaly	0.418	La Moselle
FR_A4200630	North-Atlantic Oscillation Index	0.685	Le Madon
FR_A5431010	Sum of rainfall anomaly	0.479	L' Helpe Majeure
FR_D0156510	Sum of rainfall anomaly	0.200	La Lys
FR_E3511220	North-Atlantic Oscillation Index	0.333	L' Aa
FR_E4035710	Sum of rainfall anomaly	0.612	La Seine
FR_H0400010	Snow melt	0.522	La Besbre
FR_K1503010	Sum of rainfall anomaly	0.552	L' Alagnon
FR_K2523010	Sum of rainfall anomaly	0.818	La Dore
FR_K2871910	Soil moisture layer 3	0.648	La Tardes
FR_K5183010	Sum of rainfall anomaly	0.418	La Vienne
FR_L0140610	Sum of rainfall anomaly	0.867	Le Taurion
FR_L0231510	Sum of rainfall anomaly	0.588	La Creuse
FR_L4010710	North-Atlantic Oscillation Index	0.673	La Rozeille
FR_L4033010	Evapotranspiration	0.903	La Grande Creuse

FR_L4220710	North-Atlantic Oscillation Index	0.697	La Petite Creuse
FR_L4411710	Sum of rainfall anomaly	0.770	L' Aveyron
FR_O5292510	Sum of rainfall anomaly	0.842	Le Viaur
FR_O5572910	Sum of rainfall anomaly	0.867	La Colagne
FR_O7054010	Evapotranspiration	0.903	Le Lot
FR_O7101510	Soil moisture layer 1	0.758	La Truyere
FR_O7101510	Soil moisture layer 2	0.758	La Lander
FR_O7272510	Evapotranspiration	0.333	Le Bes
FR_O7354010	Soil moisture layer 3	0.770	La Santoire
FR_O7444010	Soil moisture layer 2	0.418	La Sumene
FR_P0364010	Soil moisture layer 1	0.164	La Maronne
FR_P0894010	Leaf Area Index	0.624	La Vezere
FR_P1502510	Leaf Area Index	0.527	La Saone
FR_P3021010	Snow melt	0.517	Le Doubs
FR_U0230010	Evapotranspiration	0.564	La Drome
FR_U2122010	Sum of rainfall anomaly	0.733	L' Ubaye
FR_V4214010	Snow melt	0.570	L' Arre
FR_X0434010	Soil moisture layer 1	0.564	Le Loup
FR_Y2015010	Soil moisture layer 3	0.879	Aitrach
FR_Y5615020	Air temperature	0.224	Eger
DE_120001440	Sum of rainfall anomaly	0.479	Elta
DE_120001470	Sum of rainfall anomaly	0.794	Tauber
DE_120001920	Air temperature	0.539	Wutach
DE_120001920	Leaf Area Index	0.539	Steina
DE_120002110	Air temperature	0.661	Hasel
DE_120003570	Sum of rainfall anomaly	0.636	Brugga
DE_120003640	Sum of rainfall anomaly	0.794	Kinzig
DE_120003750	North-Atlantic Oscillation Index	0.212	Lein
DE_120003860	Sum of rainfall anomaly	0.648	Murg
DE_120003900	Sum of rainfall anomaly	0.406	Fils
DE_120004730	Sum of rainfall anomaly	0.430	Breitach
DE_120013010	Distribution of the rainfall event	0.661	Schmutter
DE_120014390	Distribution of the rainfall event	0.673	Vils
DE_11418001	Soil moisture layer 2	0.891	Steinacher Ache
DE_11418001	Soil moisture layer 3	0.891	Trauchgauer Ach
DE_11942009	Soil moisture layer 1	0.491	Illach
DE_12183005	Soil moisture layer 3	0.830	Wertach
DE_12186003	Sum of rainfall anomaly	0.915	Geltnach
DE_12326000	Soil moisture layer 3	0.758	Vils
DE_12335001	Air temperature	0.576	Grosser Regen
DE_12405005	North-Atlantic Oscillation Index	0.709	Teisnach
DE_12445000	Soil moisture layer 1	0.733	Chamb
DE_14601004	Sum of rainfall anomaly	0.467	Kollbach

DE_15214003	Evapotranspiration	0.685	Isar
DE_15218004	Evapotranspiration	0.479	Schronbach
DE_15243001	Soil moisture layer 1	0.515	Strogen
DE_15243001	Soil moisture layer 2	0.515	Grosse Vils
DE_15993001	Soil moisture layer 2	0.515	Gaissa
DE_16000708	Soil moisture layer 1	0.576	Ilz
DE_16312008	Soil moisture layer 3	0.758	Mitternacher Oh
DE_16825002	Sum of rainfall anomaly	0.515	Reschwasser
DE_17215007	Sum of rainfall anomaly	0.648	Osterbach
DE_17345002	Distribution of the rainfall event	0.541	Steinbach
DE_17404000	Leaf Area Index	0.552	Rottach
DE_17425000	Soil moisture layer 2	0.564	Attel
DE_17466007	Soil moisture layer 1	0.673	Isen
DE_17466007	Soil moisture layer 2	0.673	Tiroler Achen
DE_17468002	Distribution of the rainfall event	0.600	Traun
DE_18196000	Sum of rainfall anomaly	0.697	Saalach
DE_18216005	Soil moisture layer 3	0.394	Stoisser Ache
DE_18346000	Soil moisture layer 3	0.552	Untere Steinach
DE_18381500	Distribution of the rainfall event	0.602	Roter Main
DE_18454003	Leaf Area Index	0.612	Rodach
DE_18483500	Leaf Area Index	0.745	Baunach
DE_18642003	Snow melt	0.515	Sinn
DE_18646809	Soil moisture layer 1	0.915	Lohr
DE_24118500	Leaf Area Index	0.806	Elsava
DE_24123000	Sum of rainfall anomaly	0.636	Schwesnitz
DE_24140509	Soil moisture layer 3	0.636	Gersprenz
DE_24186000	Soil moisture layer 3	0.588	Kinzig
DE_24482003	Sum of rainfall anomaly	0.442	Nidder
DE_24522006	Soil moisture layer 1	0.442	Lahn
DE_24752006	Distribution of the rainfall event	0.632	Ohm
DE_56122008	Soil moisture layer 2	0.527	Salzboede
DE_24762653	Sum of rainfall anomaly	0.600	Cleebach
DE_24784259	Air temperature	0.612	Solmsbach
DE_24861407	Soil moisture layer 1	0.697	Aar
DE_25810558	Soil moisture layer 1	0.648	Ulster
DE_25810558	Soil moisture layer 2	0.648	Fulda
DE_25822808	Sum of rainfall anomaly	0.418	Eder
DE_25831059	Soil moisture layer 1	0.564	Schwalm
DE_25832357	North-Atlantic Oscillation Index	0.479	Hase
DE_25850257	Leaf Area Index	0.527	Oker
DE_25880305	Soil moisture layer 3	0.552	Sieber
DE_41450056	Sum of rainfall anomaly	0.636	Iilme
DE_42350057	Sum of rainfall anomaly	0.855	Innerste

DE_42810204	Soil moisture layer 1	0.915	Wumme
DE_42882806	Sum of rainfall anomaly	0.491	Klinbach
DE_3637101	Soil moisture layer 2	0.248	Nims
DE_4823104	Snow melt	0.646	Dhron
DE_4882168	Distribution of the rainfall event	0.382	Uessbach
DE_4884110	Soil moisture layer 2	0.927	Schwarzwasser
DE_4886122	Evapotranspiration	0.685	Striegis
DE_4945108	North-Atlantic Oscillation Index	0.758	Floeha
DE_23750306	Air temperature	0.297	Weisse Elster
DE_26280854	Leaf Area Index	0.345	Engnitz
DE_26760306	North-Atlantic Oscillation Index	0.539	Werra
DE_26840507	North-Atlantic Oscillation Index	0.576	Nahe
DE_563790	Sum of rainfall anomaly	0.709	Hasel
DE_567320	Air temperature	0.358	Truse
DE_568140	Sum of rainfall anomaly	0.673	Felda
DE_576400	Sum of rainfall anomaly	0.867	Ulster
DE_252460	Sum of rainfall anomaly	0.697	Hörsel
DE_420020	Snow melt	0.522	Leine
DE_421620	Sum of rainfall anomaly	0.806	Loquitz
DE_422000	Soil moisture layer 1	0.697	Ilm
DE_425120	Soil moisture layer 1	0.612	Unstrut
DE_426000	Sum of rainfall anomaly	0.636	Gera
DE_427010	Sum of rainfall anomaly	0.891	Zorge
DE_429010	North-Atlantic Oscillation Index	0.673	Berkel
DE_447000	Leaf Area Index	0.309	Glomma
DE_572010	Sum of rainfall anomaly	0.685	Jøra
DE_572920	Soil moisture layer 1	0.358	Ogna
DE_573010	Evapotranspiration	0.673	Etneelv
DE_574210	Leaf Area Index	0.479	Fusta
DE_575500	Sum of rainfall anomaly	0.467	Kjerringå
NL_1000	Leaf Area Index	0.418	Lakselv
NO_1702008	Sum of rainfall anomaly	0.685	Lakså
NO_1702033	Air temperature	0.758	Dee
NO_1727004	Soil moisture layer 2	0.588	Allan Water
NO_1741001	Soil moisture layer 1	0.382	Tweed
NO_1852001	Soil moisture layer 2	0.709	South Tyne
NO_1857002	Soil moisture layer 2	0.576	Bedburn Beck
NO_1862001	Sum of rainfall anomaly	0.697	Greta
NO_1866001	Distribution of the rainfall event	0.745	Dove
UK_12001	Sum of rainfall anomaly	0.273	Harpers Brook
UK_18001	Distribution of the rainfall event	0.418	Kym
UK_21006	Sum of rainfall anomaly	0.806	Thet

UK_23004	Distribution of the rainfall event	0.395	Coln
UK_24004	Distribution of the rainfall event	0.529	Mole
UK_25006	Leaf Area Index	0.721	Lymington
UK_28008	Air temperature	0.600	Torridge
UK_32003	North-Atlantic Oscillation Index	0.503	Frome(Bristol)
UK_33012	Soil moisture layer 1	0.503	Teme
UK_33019	Soil moisture layer 3	0.345	Wye
UK_39020	Soil moisture layer 2	0.661	Cynon
UK_39054	Soil moisture layer 2	0.661	Cothi
UK_42003	Soil moisture layer 3	0.442	Weaver
UK_50002	Sum of rainfall anomaly	0.539	Findhorn
UK_53006	Leaf Area Index	0.406	Ribble
UK_54008	Leaf Area Index	0.552	Kinnel Water
UK_55026	North-Atlantic Oscillation Index	0.709	Nith
UK_57004	Air temperature	0.333	Dulnain